REPORT 1392

BORON AND ZIRCONIUM FROM CRUCIBLE REFRACTORIES IN A COMPLEX HEAT-RESISTANT ALLOY [1]

By R. F. Decker, John P. Rowe, and J. W. Freeman

SUMMARY

In a laboratory study of the factors involved in the influence of induction vacuum melting on a 55Ni-20Cr-15Co-4Mo-3Ti-3Al heat-resistant alloy, it was found that the major factor was the type of ceramic used as the crucible. Creep-rupture properties at 1,600° F and hot-workability of the ingots were improved in proportion to the increase in trace amounts of zirconium derived from reaction of the melt with zirconia crucibles. Boron derived from the usual contamination of magnesia with boron compounds was even more effective for heats melted in magnesia crucibles. Material melted in alumina crucibles with no introduction of boron or zirconium had very low strength and ductility in rupture tests and was very prone to crack during hot-working. These findings indicate that variable amounts of boron or zirconium introduced into alloys of the type considered through reaction with crucible ceramics or unknowingly in the charge have been a major cause of variability in commercial production. Moreover, it indicates that there must be minimum amounts of one or both of these elements to obtain a practical alloy. When both boron and zirconium are present in optimum amounts, better properties apparently result than can be obtained from either element alone. Too much zirconium plus boron reduces creep-rupture properties and results in poor hot-workability. Excessive boron alone also reduces hot-workability. Good metallurgical practice, therefore, requires the addition of the optimum amounts.

A microstructural investigation was conducted to establish the mechanism of the pronounced benefits of boron and zirconium. Materials with varying boron and zirconium content were exposed to creep at 1,600° F and the microstructures were analyzed by optical and electron microscopy, electron diffraction, microfractography, and hardness measurements.

The improvement in creep-rupture properties was found to result from a pronounced stabilizing effect of boron and zirconium on the grain boundaries of the alloy. The alloy with low boron and zirconium was subject to rapid agglomeration of $M_{23}C_6$ and γ' in the grain boundaries, followed by depletion of γ' and intergranular microcracking at the grain boundaries transverse to applied stress. Brittle fracture then occurred by linking of microcracks. Additions of zirconium, boron, and boron plus zirconium decreased this tendency in that order. In the absence of these elements extensive microcracking was found late in first-stage creep at relatively short time periods and fracture occurred prematurely with very little deformation. Proper amounts of boron plus zirconium delayed microcracking until after third-stage creep had started so that creep-rupture life was greatly prolonged and ductility to fracture markedly increased.

INTRODUCTION

Although melting practice has long been known to influence the properties of heat-resistant alloys, the factors involved have not been understood. Part of the lack of understanding has been due to variable and often unpredictable differences in properties with a supposedly constant melting practice.

The major reason for initiating the present investigation was to help clarify the role of vacuum melting in the production of blade alloys for the gas turbines of jet engines. Vacuum melting with resultant improved properties had been adopted quite widely for the production of such alloys, although erratic results were being obtained by producers. Neither the causes for the erratic properties nor those resulting in the improvement in properties attributed to vacuum melting were known.

During the course of investigating the role of melting practice on the high-temperature properties of a 55Ni-20Cr-15Co-4Mo-3Ti-3Al alloy, the present authors discovered that trace amounts of boron or zirconium derived from reaction of the melt with the crucible refractories improved creep-rupture properties at 1,600° F. Boron was most effective and in addition markedly improved hot-workability.

The work of Koffler, Pennington, and Richmond (ref. 1) showed benefits to both creep-rupture life and ductility of M252, Udimet 500, Inconel 700, Nimonic 90, and Waspaloy alloys from additions of boron and zirconium. The literature cites numerous cases where beneficial effects were obtained by minute additions of certain alloying elements (ref. 2). Deoxidation with certain elements, including boron and zirconium, has been reported to improve hot-workability and properties at high temperatures for nickel-base alloys (refs. 3, 4, and 5). Confirmation of effects of boron on commercial nickel-base alloys was presented by Darmara (ref. 6) and Jones (ref. 7). The effects, however, are not restricted to nickel-base alloys. Similar benefication of

[1] Supersedes NACA Technical Note 4049, "Influence of Crucible Materials on High-Temperature Properties of Vacuum-Melted Nickel-Chromium-Cobalt Alloy," by R. F. Decker, John P. Rowe, and J. W. Freeman, 1957, and NACA Technical Note 4286, "Mechanism of Beneficial Effects of Boron and Zirconium on Creep-Rupture Properties of a Complex Heat-Resistant Alloy," by R. F. Decker and J. W. Freeman, 1958.

creep-rupture properties of numerous other alloys had been established in the past. Variations in properties of alloys at high temperatures from variations in melting and deoxidation practice has long been known.

Because vacuum melting excludes exposure to air during melting and reduces oxygen and nitrogen in alloys to lower values than are typical of air melting, the investigation originally was intended to study the influence of oxygen and nitrogen as a function of the melting technique. It soon became evident that the creep-rupture properties were mainly governed by some factor other than oxygen and nitrogen. Creep-rupture properties of the experimental heats, regardless of the oxygen and nitrogen level or other melting technique variables, were markedly inferior to those considered typical of the comercially produced alloy. Because it was known that additions of boron and zirconium had the ability to improve properties, it was demonstrated that such additions to the laboratory heats did result in properties equivalent to the alloy as commercially produced. Commercial producers, however, insisted that the alloy could be made with high properties without such additions and that there must be some other factor in vacuum melting which had been overlooked in the research. Continued modifications of the melting technique, however, failed to improve the alloy to the expected level.

The Utica Drop Forge and Tool Co. (now the Utica Drop Forge and Tool Division of Kelsey-Hayes Co.) had developed adequate methods of analysis for zirconium, and their cooperation in analyzing the experimental heats disclosed that the variations which existed in properties correlated with variations in trace amounts of zirconium. The properties increased regularly with increases in the amounts of zirconium. Because zirconium was not added to the heat and was not present in the melting stock, it must have been the product of reaction between the melt and the crucible refractory. The highest strength heat, however, was no better than those on the low side of the range of values for commercially produced material.

The fact that zirconium derived from zirconia crucibles during melting explained the variations in properties prompted the decision to investigate heats made in other refractories. When heats were melted in magnesia, the refractory generally used commercially, a marked but variable improvement in properties was found, with one heat being comparable to the best commercially produced material. Heats melted in alumina had uniformly very poor properties. Moreover the hot-workability of the material melted in alumina was very poor while it was markedly better for the high-strength heats melted in magnesia.

The first thought was that magnesium derived from reaction between the melt and the magnesia was responsible for the improved properties. Neither chemical analyses nor attempts to add magnesium to heats supported this possibility. The Universal-Cyclops Steel Corp. had presented a report (ref. 1) which showed marked improvement in properties from boron and zirconium additions for a number of nickel-base titanium and aluminum heat-resistant alloys. Accordingly their assistance in analyzing for boron was obtained. Practically no boron was found in heats melted in alumina or zirconia. However, very small but significant amounts of boron were found in the heats melted in magnesia, with those heats containing the largest amounts of boron having the best properties and hot-workability. Boron compounds normally present in commercial magnesia as an impurity were the source of the boron. The responsibility of boron or zirconium derived from reaction with crucible refractories for the change in properties was verified by adding these elements to heats melted in alumina crucibles with resultant properties equivalent to the heats melted in magnesia or zirconia. A few heats were also made with simultaneous additions of both boron and zirconium.

Because of the previous difficulties producers immediately checked the first indication that trace amounts of boron derived from magnesia were responsible for improved properties. A large number of heats in which boron or zirconium were not knowingly added were quickly determined by the producers to have properties correlating with boron and/or zirconium content either derived from reaction with crucible refractories or unknowingly added in the melting stock. Accordingly it seemed to be useless to make more heats in the experimental furnace and this report is based on the relatively few heats from which the original discovery was made.

The investigation was then broadened to study microstructures to obtain information on the mechanism by which trace amounts of boron and zirconium improved creep-rupture properties and it seemed logical to study their effects on the structural characteristics which had previously been shown to control properties. It would increase knowledge of the theory of alloying and give a more basic understanding of alloy design to resist creep and rupture. In addition, it might also reveal the nature and cause of rupture in these materials.

Since it had been established that the source of the boron and/or zirconium was not important, the mechanism study was not limited to heats in which these elements had been derived from the crucible refractory. Rather, heats were chosen which contained what appeared to be optimum amounts of each element.

It is generally accepted that the favorable high-temperature properties of the nickel-base alloys hardened with titanium plus aluminum result from the precipitation of the intermetallic γ' phase within the matrix of the alloy. The γ' phase has been shown to have a face-centered cubic structure similar to that of the Ni_3Al phase of the nickel-aluminum system with a lattice parameter closely matched to that of the matrix of the alloys (refs. 8 and 9). Compositionally, the phase has been shown to dissolve titanium and is frequently referred to as $Ni_3(Al,Ti)$.

Although the creep resistance of these alloys has been attributed to the presence of γ' in fine dispersion within the matrix (refs. 8 and 10), attempts to relate the distribution of the γ' particles with the metallurgical properties have been only moderately successful to date. Frey, Freeman, and White (ref. 11) and subsequently Brockway and Bigelow (ref. 12) found that dispersion of the γ' particles in Inconel-X alloy correlated with creep-rupture properties at 1,200° F, which was low in the aging range for this alloy; however, no correlation was obtained for rupture tests at 1,500° F, which was high in the aging range. Betteridge and Smith (ref. 13) studied the relations between structure and creep properties

of several Nimonic alloys when tested high in the aging range. Highest creep-rupture properties were obtained with the greatest volume percent of γ'. Baillie (ref. 14) found that best creep resistance in Ni-Cr-Al-Ti alloys was obtained with the highest density of γ' particles.

Carbide reactions occur in the titanium- and aluminum-hardened nickel-base alloys and have been related to properties. Among the carbides identified are $M_{23}C_6$ (refs. 12, 15, and 16), M_6C (refs. 15 and 16), Cr_7C_3 (ref. 17), and TiC (refs. 15 and 16). The occurrence of a type of carbide is dependent both on the alloy content and the temperature of treatment. In general, the carbide reactions in these alloys are poorly understood. Their probable importance in controlling properties was indicated by Betteridge and Franklin (ref. 17) who established the benefits on rupture life of obtaining a high-temperature precipitate of Cr_7C_3 before creep exposure of Nimonic alloys.

This investigation was conducted at the University of Michigan Research Institute under the sponsorship and with the financial assistance of the National Advisory Committee for Aeronautics. The chemical analyses were supplied gratis by the Utica Drop Forge and Tool Division of Kelsey-Hayes Co. and the Universal-Cyclops Steel Corp. Particular credit is due Dr. W. C. Bigelow and Mr. J. A. Amy for the phase identifications, which were part of a program of research in identification of minor phases in heat-resistant alloys sponsored by Metallurgy Research Branch, Aeronautical Research Laboratory, Wright Air Development Center.

EXPERIMENTAL PROCEDURES

MELTING

The experimental heats were induction-melted in the University of Michigan vacuum-melting unit shown in figure 1. Pressures before meltdown and after pouring were less than 5 microns as measured by both Stokes and thermocouple gages. No gases were purposely added to the chamber during the melting cycle. Melt temperatures were meaured with an immersion thermocouple with one platinum and one platinum and rhodium wire. Melting cycles for all the heats are detailed in table I and figure 2.

The aim of the analysis for the basic alloy, in weight percent, for all heats was as follows:

Chromium	Cobalt	Molybdenum	Titanium	Aluminum	Manganese	Silicon	Carbon	Nickel
20.0	15.0	4.0	3.1	3.1	0.12	0.12	0.08 to 0.15	Balance

Varied amounts of boron and zirconium were added to certain heats for the purposes of the investigation.

Laboratory-grade electrolytic nickel, chromium, cobalt, and manganese melting stocks were used. The other elements were added in the form of low-carbon arc-melted molybdenum, Ti–55A bar titanium, 99.99-percent-pure ingot aluminum, 99.9-percent-pure silicon powder, sponge zirconium, nickel-boron master alloy, and powdered or chuck graphite.

The crucible refractories were alumina, zirconia, and magnesia. Pertinent data on these materials are listed in

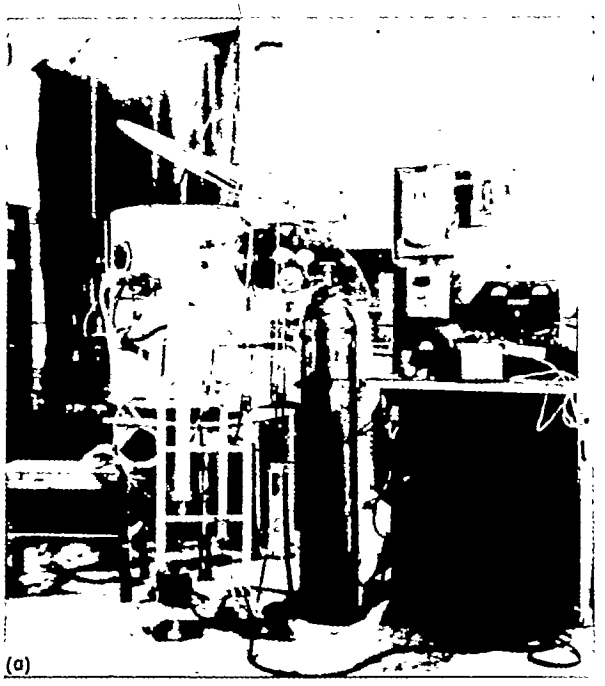

(a) External view.
(b) Internal view showing crucible, charge buckets, and ingot mold.

FIGURE 1.—University of Michigan vacuum-melting furnace.

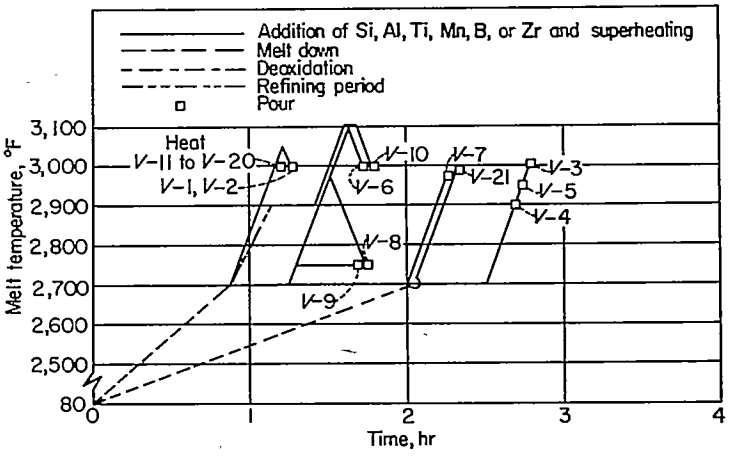

FIGURE 2.—Melting cycles used in study of effect of melting variables on high-temperature properties of experimental alloy.

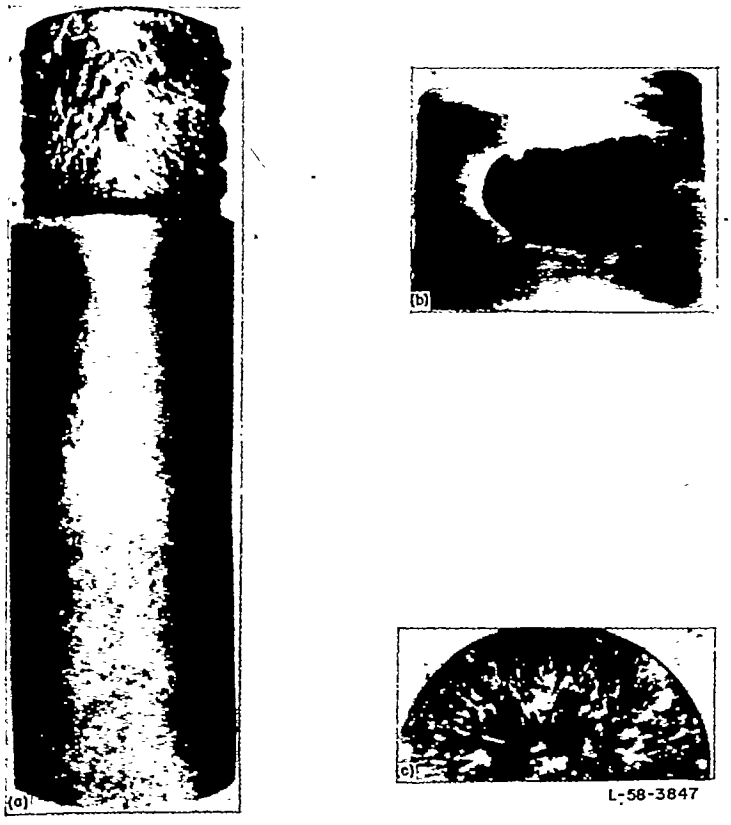

(a) As-cast ingot 9 inches long with 2.5-inch diameter; weight, 10 pounds.
(b) Section of hot top showing isolation of pipe to hot top.
(c) Macrostructure of ingot section.

FIGURE 3.—Typical as-cast ingot from experimental heats.

table II with chemical compositions obtained from the suppliers.

Ten-pound heats were poured into an open-bottomed copper mold which rested on a massive copper block. An insulating refractory ring mounted in the top of the copper mold served as the hot top. An as-cast ingot, a hot-top section, and the ingot structure are shown in figure 3.

HOT-WORKING AND HEAT TREATMENT

Most of the 10-pound ingots were processed as follows:

(1) Homogenized 1 hour at 2,300° F, air-cooled.

(2) Surface-ground.

(3) Rolled at 2,150° F to ⅞-inch bar stock using 22 passes with 21 reheats of 10 minutes between passes. The last pass was a 7-percent reduction followed by air-cooling.

Heats V–20, V–21, and V–24 were not homogenized or ground, and heats V–18 and V–19 were rolled at 2,000° F to ⅞-inch bar stock using 36 passes with 35 reheats.

All of the stock was solution-treated at 2,150° F for 2 hours and then air-cooled. The rupture tests were conducted on the material in this condition. In conducting the tests the specimens were preheated for 4 hours at 1,600° F before the stress was applied. The 2-hour treatment at 2,150° F also was applied prior to aging experiments.

The evaluation of hot-workability was limited to visual observations of the type and degree of cracking during rolling and to comparison of the limitations during working necessary to obtain usable bar stock.

CHEMICAL ANALYSIS

Samples for chemical analysis were cut from the midpoint of the as-rolled bar stock. This metal was originally in the center of the ingot. Titanium, aluminum, molybdenum, chromium, cobalt, manganese, magnesium, copper, iron, and zirconium were determined spectographically through the courtesy of the Utica Drop Forge and Tool Corp. Carbon, sulfur, and phosphorus were determined by chemical analysis of machined chips. Residual calcium, iron, copper, and magnesium were checked spectrographically on heats V–13, V–20, and V–21. The difficult and time-consuming analyses for boron, provided gratis by the Universal-Cyclops Steel Corp., were made by a wet-chemical method.

SPECIMENS FOR DETERMINING PROPERTIES AT HIGH TEMPERATURES

Specimens having a 0.250-inch diameter by 1-inch long gage section were machined from the heat-treated bar stock. The original ⅞-inch stock was quartered lengthwise to provide specimen blanks from each quarter. The high-temperature properties of the experimental heats were evaluated by rupture tests on these specimens at 1,600° F and 25,000 psi. In part of the tests creep data were taken on the specimens using an optical extensometer having a sensitivity of 0.000005 inch per inch for strain measurements.

MECHANISM STUDIES

The mechanism studies were concentrated on the four heats with the largest differences in properties from the trace-element effects. Heat V–15 (see table III) was selected as representative of material with very low boron and zirconium. A relatively high zirconium content for the series of heats available was represented by heat V–6. Heat V–12 was representative of a fairly high boron content and heat V–14 had significant amounts of both boron and zirconium.

Samples from these heats were subjected to extensive microstructural studies using both optical and electron microscopic techniques. Phase identifications were carried out using electron diffraction on extraction replicas. To define the influence of boron and zirconium it was found necessary to age samples with and without stress. The samples aged under stress were obtained by interrupting creep-rupture tests. Several features of the microstructure had to be evaluated by counting techniques. The details of the procedures are presented in the following sections.

Procedures with aged specimens.—Small samples were heated in a muffle furnace for time periods up to 500 hours at 1,600° F to provide specimens with structural changes characteristic of those produced in the absence of stress. These samples were subjected to hardness tests as well as to microstructural examination. Diamond pyramid hardness (DPH) was measured with a 50-kilogram load. Three impressions were made on each sample. Analysis of testing variability established that in the range of 200 to 340 DPH a difference of 7 DPH was significant while in the range of 340 to 400 DPH a difference of 9 DPH was required to be significant.

Specimens aged under stress were obtained by starting tests at 1,600° F in the same manner as for rupture tests. The objective was to obtain specimens showing the microstructural changes occurring during the course of the creep-

rupture tests. When the required time had elapsed, the load was released and the specimen was immediately removed from the furnace to cool in air. Creep data were taken during these aging treatments so that the structural changes could be expressed as a function of deformation as well as of time. Fractured rupture specimens were also examined. In one series, the stresses were adjusted to give approximately equal creep rates in all four heats.

All specimens were sectioned lengthwise to present surfaces for examination which were parallel to both the direction of rolling and the direction of the stress for specimens subjected to creep.

Light microscopy.—Metallographic samples were mechanically polished through wet papers to 600 grit and then the majority were polished on wet cloths with Linde A and Linde B powders. A few, as noted in the figures, were electropolished after 600 grit paper in a solution of 10 parts of 70-percent perchloric acid and 90 parts of glacial acetic acid at 50 volts with a current density of 2 amperes per square inch. Cyclic polishing of 5 seconds on and 5 seconds off was employed for a total period of electrolysis of 30 seconds.

The procedure and etchant developed by Bigelow, Amy, and Brockway (ref. 18) was used to reveal best the precipitating phases at 100, 1,000 and 2,000 diameters. This involved etching electrolytically at 6 volts and a current density of 0.8 ampere per square inch for periods of 5 to 7 seconds, depending upon the sample condition. The etchant composition was 12 parts of 85-percent phosphoric acid, 47 parts of 96-percent sulfuric acid, and 41 parts of 70-percent nitric acid.

Electron microscopy.—Metallographic samples were mechanically polished through wet papers to 600 grit. This polishing was followed by electropolishing using the procedure described in the previous section on light microscopy.

Etching for examination with the electron microscope was accomplished with the etchant described under light microscopy with the etching time reduced to periods of 1 second to 5 seconds.

After etching, collodion replicas of the metallic surface were made. These were shadowed with palladium to increase contrast and reveal surface contours. Polystyrene latex spheres approximately 3,400 angstrom units in diameter were placed on the replicas prior to shadowing to indicate the angle and direction of shadowing and to provide an internal standard for measurement of magnification. The micrographs reproduced in this report are copies of direct prints from the original negatives; consequently, the polystyrene spheres appear black and the "shadows" formed by the palladium appear white.

Quantitative structural evaluations and techniques.—During the course of the structural studies it became evident that certain features were related to properties. The most significant were microcracks formed in the grain boundaries, depletion of the γ' phase from the matrix adjacent to the grain boundaries, "nodules" of precipitates which formed within the grains, the dispersion of γ' particles in the matrix, and cracks originating at the surface.

In order to make the trends and comparisons quantitative, counts were made of the number of depleted grain boundaries, microcracks, and nodules in an 0.008-square-inch area using a magnification of X1,000 on mechanically polished and etched specimens. An area of 0.008 square inch was surveyed as eight strips, each 0.2 by 0.005 inch. In the case of interrupted creep tests, the strips were longitudinal to the specimen axis at the center of the specimen and at the minimum cross section. In ruptured samples, the strips were again longitudinal, starting in the grains at the fracture surface and progressing away from the fracture.

A depleted grain boundary was counted when a clear, white strip of matrix free of γ' particles was clearly seen along a grain boundary.

Microcracks were easily distinguishable by their blackness which was in complete contrast with all other intragranular and intergranular features of the samples. Early doubts about the identity of microcracks were eliminated when electropolishing enlarged and accentuated these black voids and when fins on electron-microscope replicas were found where these had filled the microcracks. Each distinct microcrack was counted. A crack had to be 1 micron in length to be counted because shorter microcracks were not distinguishable from carbide-matrix interfaces. Counting of nodules was arbitrarily limited to those more than 5 microns in diameter.

Intergranular surface cracks were counted on mechanically polished specimens by traversing longitudinal section surfaces at 500 diameters. This cracking was found to be quite uniform over the reduced section of the specimens. In the case of interrupted creep specimens the cracks were counted over the center 0.75 inch, while in ruptured samples counts were made for 0.50 inch starting at the fracture. Intergranular cracks penetrating less than 0.003-inch deep were not counted.

A rough measure of γ' dispersion was obtained by the surface density of γ' particles in electron micrographs. An area large enough to contain at least 100 particles was surveyed at 12,000 diameters.

The above techniques allow quantitative comparison of the tendency of the four heats to undergo structural changes. It is recognized that percent of grain-boundary area cracked, percent of grain-boundary area depleted, volume percent of nodules, and volume percent and interparticle distance of γ' would be fundamentally more sound quantities for correlation. However, these more refined and time-consuming techniques would not alter the conclusions of this paper and, therefore, were not considered necessary.

Phase identification.—The extraction-replica technique of Fisher (ref. 19) was used to identify precipitated phases by electron diffraction. In this procedure a replica is placed on the surface of the sample and the metal surface then selectively etched so that the precipitate of interest is left adhering to the surface of the replica.

For extraction of intragranular γ', the initial specimen preparation was identical to the electropolishing and etching used for electron metallography. The specimen preparation for extraction of intragranular precipitates consisted of electropolishing and then electrolytically etching for 15 minutes in 1 part 85-percent phosphoric acid to 4 parts water in order to remove the γ' particles.

For extraction of intergranular particles, the microfractographic techniques of Plateau, Henry, and Crussard (ref. 20)

proved adequate. Specimens were cooled in liquid nitrogen and then fractured using a hammer and chisel, the fracture being intercrystalline. The fracture surface was then etched with the same procedure described above for electron microscopy.

Carbon replica films were deposited on the prepared surfaces by the method of Bradley (ref. 21) and were backed by thicker supporting films of collodion. The surfaces were then etched electrolytically in a solution of 1 part 85-percent phosphoric acid to 4 parts water until the compound replica films separated from the surface. The films were transferred to the surface of clean distilled water and allowed to wash by diffusion, picked up on nickel screens, washed again, and the collodion backing films dissolved from the carbon films with amyl acetate by the method of Fullam (ref. 22). The replicas were then shadowed with aluminum to provide an internal standard for interplanar distances. Electron-diffraction patterns were obtained from the particles by selected area electron-diffraction techniques on the microscope. Electron micrographs were obtained from the replicas in an electron microscope to show the phases subjected to electron diffraction.

RESULTS

The data obtained gave two main results: (1) The establishment of the marked improvement of creep-rupture properties and hot-workability from zirconium or boron derived from reaction between the melt and crucible refractories; and (2) the delineation of the mechanisms by which boron and/or zirconium improved the creep-rupture properties.

INFLUENCE OF CRUCIBLE REFRACTORY

The poorest hot-workability and the lowest rupture life and ductility were found for heats melted in alumina crucibles. Better properties were found for heats melted in zirconia and still better for those melted in magnesia. In presenting the results, the chemical composition of the melted heats will be discussed first because the cause for the observed property effects was found through the chemical analyses. The hot-workability of the heats will be presented second and the creep-rupture properties third.

Chemical composition.—The composition variables of primary interest in this investigation proved to be boron and zirconium. The levels investigated varied depending on the type of crucible employed for the melting and whether deliberate trace-element additions were made to the heats. The results of chemical analyses on heats melted with no deliberate additions of boron or zirconium (see table III) indicate the following ranges of analysis for these elements:

Type of crucible	Range in analysis, weight percent	
	B	Zr
Alumina	0.0002 to 0.0003	<0.01
Zirconia	.0004 to 0.0005	<0.03 to 0.19
Magnesia	.0004 to 0.0017	<0.01

In order to verify that the boron and/or zirconium were the controlling variables independent of their source and to extend the study to higher levels than were obtainable by reaction with the crucibles, additional heats were made in all three types of crucibles with deliberate additions of boron and/or zirconium during melting. This increased the range of boron up to 0.0089 percent and gave heats melted in alumina for which essentially none of the boron and/or zirconium was derived from reaction with the crucible.

The lower limit of sensitivity for zirconium during the analysis of heats V–1 through V–10 was 0.03 percent. The sensitivity had improved to 0.01 percent for heats V–11 through V–24.

Although the majority of the heats had carbon contents in the range of 0.05 to 0.12 percent, several heats contained carbon levels above this range. Titanium and aluminum also varied because of the wide range of melting techniques used. In addition, the degree of reliability of analyses for magnesium, calcium, and copper is uncertain. The results obtained, however, did not disclose significant variations for these elements.

Hot-workability.—Working conditions for the alloy were found to be limited in temperature range, amount of reduction per pass, and the reheat time between passes because of the tendency for cracking to occur. The most successful practice found for the heats with less than 0.01 percent zirconium and less than 0.001 percent boron was to roll from 2,150° F using approximately 7-percent reductions per pass with a 10-minute reheat at 2,150° F between passes. Therefore, this practice was adopted for all rolling except for heats V–18 and V–19, which were rolled from 2,000° F with smaller reductions to avoid the hot-shortness at temperatures above 2,000° F which was related to combined content of boron and zirconium.

Observation of hot-working revealed that two distinctly different types of cracking occurred. The first type was a severe internal rupturing of the stock. The appearance of one of these ruptures is shown in figure 4. The second

(a) Ingot after three passes at 2,150° F.
(b) ⅞-inch bar stock rolled from cracked section of ingot shown in (a). Large cracks could not be ground out.

FIGURE 4.—Internal rupture in heat V–14 with 0.0088 percent boron and 0.01 percent zirconium and resultant bar stock after continued hot-rolling.

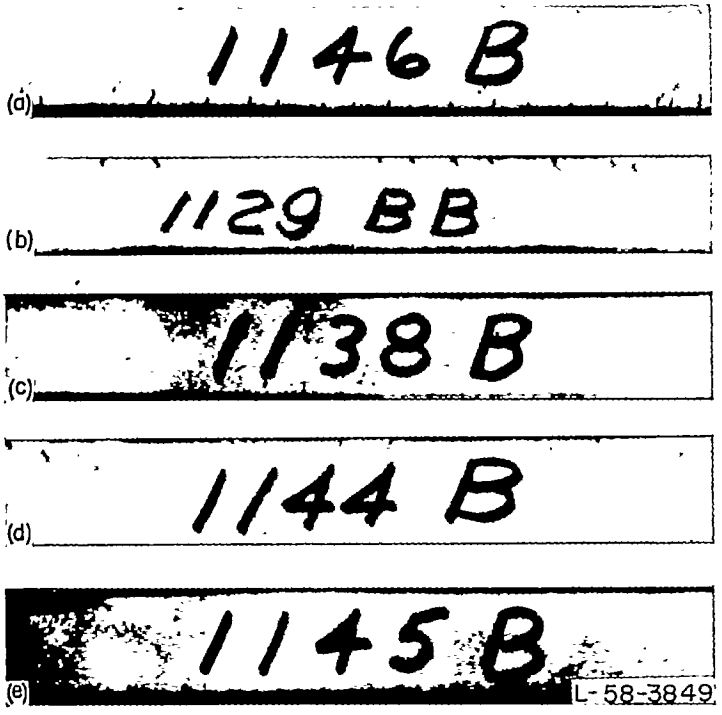

(a) Heat V–13 with 0.0003 percent boron and less than 0.01 percent zirconium.
(b) Heat V–1 with 0.09 percent zirconium with no boron addition.
(c) Heat V–6 with 0.19 percent zirconium and 0.0004 percent boron.
(d) Heat V–11 with 0.0017 percent boron and less than 0.01 percent zirconium.
(e) Heat V–12 with 0.0089 percent boron and less than 0.01 percent zirconium.

FIGURE 5.—Effect of boron or zirconium content on corner cracking of experimental heats when rolled to ⅞-inch-square bars at 2,150° F.

type was corner cracking (fig. 5) which occurred after the round ingot had been broken down to square bar stock in the rolling mill. It was found that both types of cracking were related to trace element content.

The 2,300° F treatment included in the standard rolling practices was first adopted using heats with no boron in the belief that it would minimize corner-cracking problems during rolling by homogenizing the as-cast ingot. It is possible that this treatment magnified the internal-rupture problem in heats to which boron was added. The introduction of the 2,300° F treatment was based on experience with one of the higher zirconium heats and it is now considered that the zirconium and not the heat treatment was responsible for the improved hot-workability.

The cracking characteristics are presented in terms of the boron and/or zirconium contents alone. The relationship of these elements to crucible refractories will be discussed in detail in the subsequent section on rupture properties.

Internal cracking during rolling: The relationships governing internal rupturing during ingot breakdown were:

(1) The base alloy as melted in alumina was not subject to internal rupturing.

(2) Zirconium content of the heats melted in zirconia or alumina without boron additions apparently did not introduce internal rupturing. The relation held up to a zirconium content of 0.19 percent (heat V–6).

(3) Increasing boron content in the presence of less than 0.01 percent zirconium did introduce internal rupturing. This was first noticed in the finished bar stock of heat V–12 (0.0089 percent B) which exhibited some small voids along the center line resulting from internal rupture during ingot breakdown.

(4) The presence of both boron and zirconium in the amounts investigated markedly increased internal rupturing during ingot breakdown. Figure 4 illustrates the severity of this in heat V–14 which contained 0.0088 percent boron and 0.01 percent zirconium. Thus, the small increase in zirconium content from less than 0.01 percent (the lower limit of analysis) in heat V–12 to a definite 0.01 percent in heat V–14 in the presence of a boron content of near 0.009 percent was enough to intensify internal rupturing. In general, the severity of the internal rupturing in the heats containing 0.0069 to 0.0090 percent of boron (heats V–12, V–14, V–17, V–18, and V–19) increased with zirconium content in the range from less than 0.01 to 0.09 percent of zirconium. Heats V–18 (0.0069 percent B and 0.09 percent Zr) and V–19 (0.0090 percent B and 0.04 percent Zr) were very hot-short during the first passes in the standard rolling schedule.

(5) The time of internal rupturing in the rolling cycle was a function of the boron and zirconium levels. In heat V-14 (0.0088 percent B and 0.01 percent Zr), internal rupturing was limited to the first three passes at 2,150° F where it occurred along the as-cast grain boundaries. Once the original as-cast structure was recrystallized, internal rupturing ceased and the stock was reduced to ⅞-inch bar stock successfully with the standard rolling procedure. However, in heat V-18 (0.0069 percent B and 0.09 percent Zr) and heat V-19 (0.0090 percent B and 0.04 percent Zr), internal rupturing persisted after recrystallization of the as-cast grains. In order to minimize this rupturing throughout the rolling cycle, the rolling temperature was lowered to 2,000° F and the reductions per pass to 3 percent. With this procedure it was possible to obtain some useful stock for rupture-testing.

Corner cracking during rolling: After the round ingots had been broken down to 1⅜-inch squares in the rolling mill, shallow corner cracking occurred in some of the experimental heats. These cracks could be ground out between passes rather easily but reoccurred during subsequent passes. The severity of this cracking was variable; some of the heats were very malleable with no corner cracking while others underwent cracking with each pass.

As seen in figure 5, the relationships governing corner cracking during rolling of the bar stock were:

(1) In heats melted in alumina or zirconia crucibles with no boron additions, cracking decreased with increasing zirconium content (figs. 5(a) and 5(b)).

(2) In heats with less than 0.01 percent zironium (melted in alumina or magnesia crucibles), cracking decreased with increasing boron content (figs. 5(d) and 5(e)).

(3) Corner cracking was not a problem in the heats containing moderate amounts of both boron and zirconium (fig. 5(c)).

Stress-rupture properties.—The evaluation of the influence of boron and/or zirconium was based on creep-rupture tests at 1,600° F and 25,000 psi. (See table IV and figs. 6 through 12.) The data obtained showed that rupture time and ductility increased with zirconium content and

that boron was more effective than zirconium. The presence of certain amounts of both boron and zirconium gave even higher strength, although the properties fell off when zirconium increased above 0.01 percent in the presence of 0.0069 to 0.0090 percent of boron. A major result of the experiments was the demonstration that properties correlated with boron and zirconium contents whether these were derived from reaction with the crucible refractory or deliberately added to the heats.

Zirconium from zirconia crucibles: The rupture properties of heats V-1 to V-10 correlated with the amount of zirconium in the heats (figs. 6 and 7), and the rupture life increased regularly with increased zirconium up to 0.19 percent. The rupture life, however, seemed to be dependent on the amount of titanium plus aluminum in the heats, as is indicated in figure 6 by the arbitrary grouping of the data for heats with less than or more than 6.5 percent of titanium plus aluminum. Elongation and reduction-of-area values increased when the heat contained up to about 0.10 percent zirconium independent of the titanium-plus-aluminum content, except in the cases of the high values for the high-carbon heats V-8, V-9, and V-10 where the high carbon contents appear to increase ductility of the alloy in rupture tests.

Heats V-1 through V-10 were all melted in zirconia crucible with no zirconium added. The zirconium contents represented the variable amounts introduced into the heats as a result of reaction between the melts and the crucible refractories. The variable amounts of zirconium presumably were due to the wide ranges in refining practice, deoxidation practice, superheat temperature, pouring temperature, and time of melting used in making the heats. These variables represented widely varying conditions for reaction between the melt and the zirconia. The amount of zirconium derived from the crucible was, however, a more complicated factor than these melting variables inasmuch as no relations to the melting technique could be discerned in the data.

The important result of these tests was the determination that the zirconium content was the overwhelming variable and wide variations in melting technique had, at most, minor effects. The heats melted in alumina had still lower properties than the poorest heat melted in zirconia. Analytical procedures were not sufficiently sensitive to detect

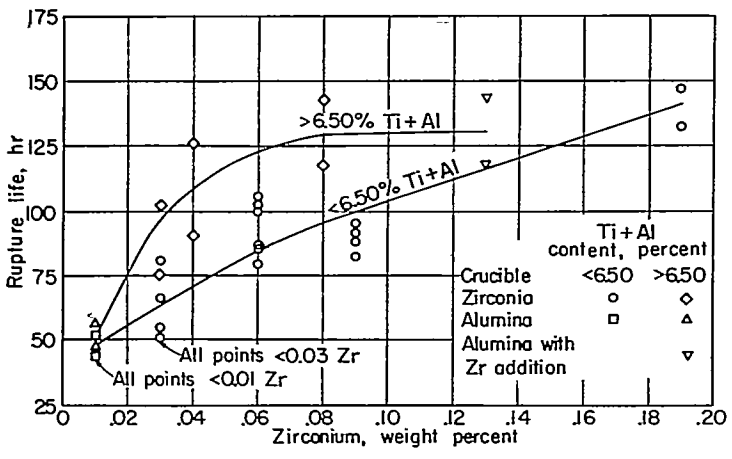

FIGURE 6.—Effect of zirconium content on rupture life at 1,600° F and 25,000 psi of experimental heats melted in zirconia or alumina with very low boron.

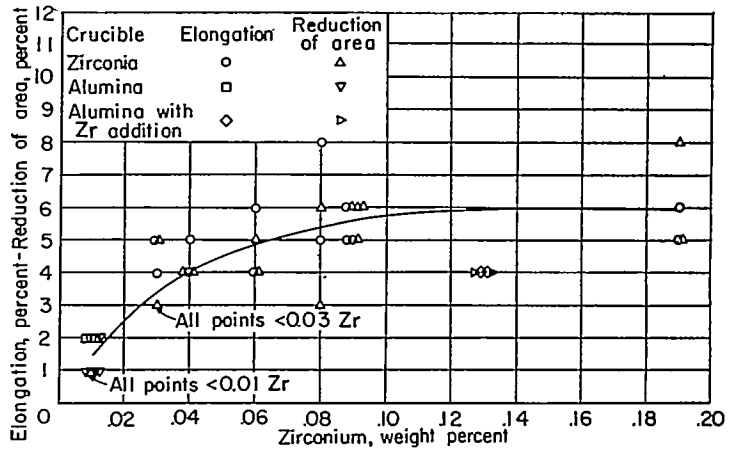

FIGURE 7.—Effect of zirconium content on ductility in rupture tests at 1,600° F and 25,000 psi of experimental heats melted in zirconia or alumina with very low boron.

the difference in zirconium contents of the heats melted in alumina and the lowest zirconium heats melted in zirconia. Presumably there were slight benefits from zirconium for amounts less than 0.03 percent, the lower limit of analytical sensitivity when heats V–1 through V–10 were analyzed. Confirmation of the controlling effect of zirconium independent of the other variables was obtained with heat V–16 by adding zirconium to a heat melted in alumina. The rupture times and ductilities (figs. 6 and 7) agreed with those expected on the basis of zirconium content within the limits of the experimental variables.

Boron from magnesia crucibles: The determination that zirconium derived from the zirconia crucibles was the controlling factor in the creep-rupture properties suggested that other refractories should be investigated as crucible materials. Accordingly, heats V–11, V–20, and V–21 were melted in magnesia crucibles. Heats V–11 and V–20 had rupture times of about 200 hours (fig. 8) in comparison with heat V–21 at about 100 hours. The ductility of all three heats (fig. 9) was in the range of 3 to 5 percent. The 100 hours for rupture for heat V–21 was equivalent to that for material with up to 0.10 percent zirconium based on the results for heats melted in zirconia (fig. 6). Heats V–11 and V–20 had

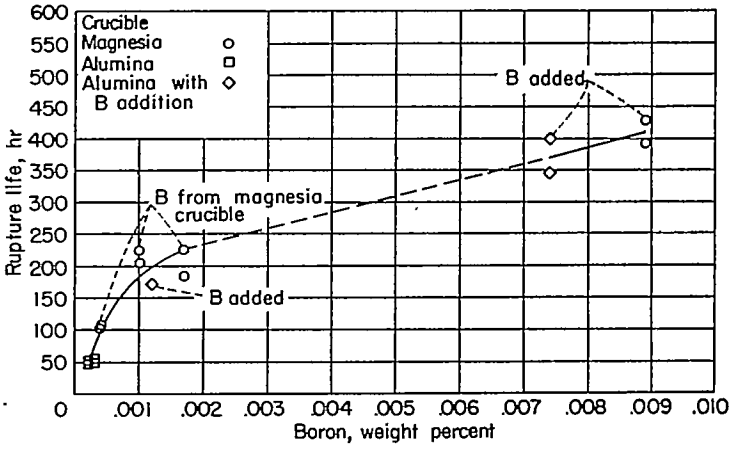

FIGURE 8.—Effect of boron content on rupture life at 1,600° F and 25,000 psi of experimental healts melted in alumina or magnesia with less than 0.01 percent zirconium.

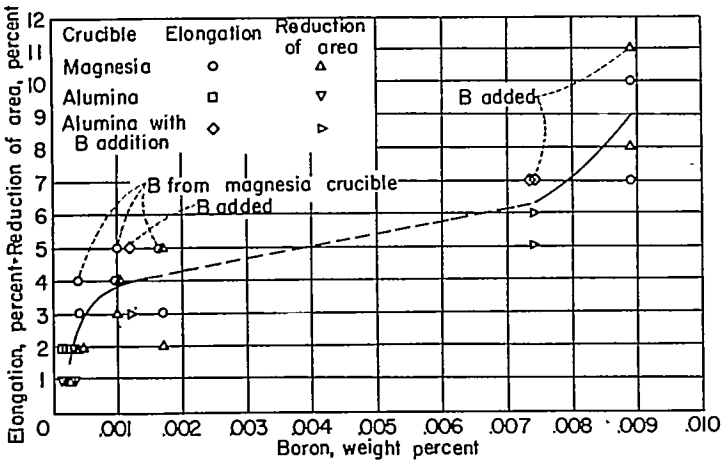

FIGURE 9.—Effect of boron content on ductility in rupture tests at 1,600° F and 25,000 psi of experimental heats melted in alumina or magnesia crucibles with less than 0.01 percent zirconium.

higher rupture strength than any of the heats melted in zirconia.

Analysis of the heats indicated that the boron contents of heats melted in magnesia were 0.0004 percent in heat V–21, 0.0010 percent in heat V–20, and 0.0017 percent in heat V–11. In view of the known powerful improving effect of boron on the properties of the alloy, this suggested that the boron was the controlling factor. This was confirmed by adding boron to heat V–24 melted in alumina (see figs. 8 and 9). Heat V–17, also melted in alumina, contained considerably more boron than was derived from crucible reaction in other heats as a result of a boron addition. This confirmed the marked improvement from boron for heats melted in alumina. Furthermore, it seemed to correlate with the expected effect of boron based on the results from heat V–12 in which boron had been added while melting in magnesia.

The boron in the heats melted in magnesia apparently came from the boron compounds which were present in the crucible. When the presence of boron in the heats melted in magnesia was first established, a check of the literature indicated that commercial magnesia is normally contaminated with boron compounds. The producer of the crucibles furnished the analysis shown in table II. The highest boron heat was the first one made in a fresh crucible. The amount of boron derived from the crucible decreased with succeeding heats. (Compare heats V–20 and V–21.)

The general agreement in properties for heats melted in alumina with those for heats melted in magnesia for the same boron content indicated that magnesia was contributing very little to improved characteristics other than by adding boron. It was first thought that magnesium might be involved since this element is often used as a deoxidizer with beneficial effects; however, there was practically no indication that magnesium was having much effect in the heats. Attempts to add magnesium during vacuum-melting proved inconclusive because of the very rapid evolution of magnesium as a vapor.

Alumina crucibles: Alumina crucibles were introduced into the program to check further the role of refractories. Any increase in aluminum content as a result of reaction between the crucible and the melt would be negligible in view of the large aluminum content of the heats. Two of the heats melted in alumina (V–13 and V–15) had the lowest strengths and ductilities of all the heats melted as was to be expected from the very low amounts or absence of zirconium and boron. For this reason the properties of heats V–13 and V–15 have been used in figures 6 through 9 to show the effects of very low amounts of these trace elements. As previously discussed, adding zirconium or boron to heats melted in alumina resulted in properties to be expected from the zirconium or boron contents.

So far as is known the alumina crucible did not contain sufficient boron or zirconium (table II) to expect a measurable addition of these elements to the heats. This seems verified by the analyzed compositions of the heats. The silicon dioxide in the alumina may have resulted in a very slight increase in silicon content of the heats.

Boron-plus-zirconium effects: In view of the pronounced improvement in properties obtained from boron derived from magnesia crucibles or by addition of boron to heats melted in magnesia, boron was added to a heat melted in zirconia (heat V–14). This heat had the highest rupture strength (646 hours) and ductility (14-percent elongation) of any of the heats made. However, heats V–18 and V–19, made in alumina with boron and zirconium additions, did not have as high properties as did heat V–14. The analyzed borons for the three heats ranged from 0.0069 to 0.0090 percent. The zirconium content of heat V–14 was only 0.01 percent while it was 0.04 and 0.09 percent for heats V–19 and V–18. When the rupture times and ductilities were plotted as a function of zirconium content for heats with boron contents of 0.0069 to 0.0090 percent (fig. 10), an apparent optimum amount of zirconium of approximately 0.01 percent is indicated.

It should be noted, as was remarked earlier, that heats V–18 and V–19 had to be rolled from 2,000° F rather than from 2,150° F because of hot-shortness. In addition, it is possible that use of the 2,300° F homogenizing treatment before rolling had an adverse effect when the boron and zirconium level was comparatively high. Therefore, any conclusions drawn from figure 10 should be qualified by recognizing that the differences in hot-working temperatures and the use of the 2,300° F treatment could have influenced the properties.

Comparison with commercial material: The basic alloy studied for the investigation was based on the commercial alloy Udimet 500 developed by the Utica Drop Forge and Tool Corp. Figure 11 shows a band which would encompass the curves of stress against rupture time at 1,600° F as reported for the alloy by the manufacturer. The rupture time for heat V–13 is shown in figure 11 to indicate the low strength of the experimental heats made in alumina crucibles with resultant very low zirconium and boron. The best heat made in zirconia (heat V–6 with 0.19 percent zirconium) had strength near the lower side of the band for commercial heats. Heat V–11, the highest boron heat melted in magnesia, was just within the band. When boron was added to a heat melted in magnesia (heat V–12) to bring the boron up to 0.0089 percent, properties near the upper side of the band were obtained. The strongest heat

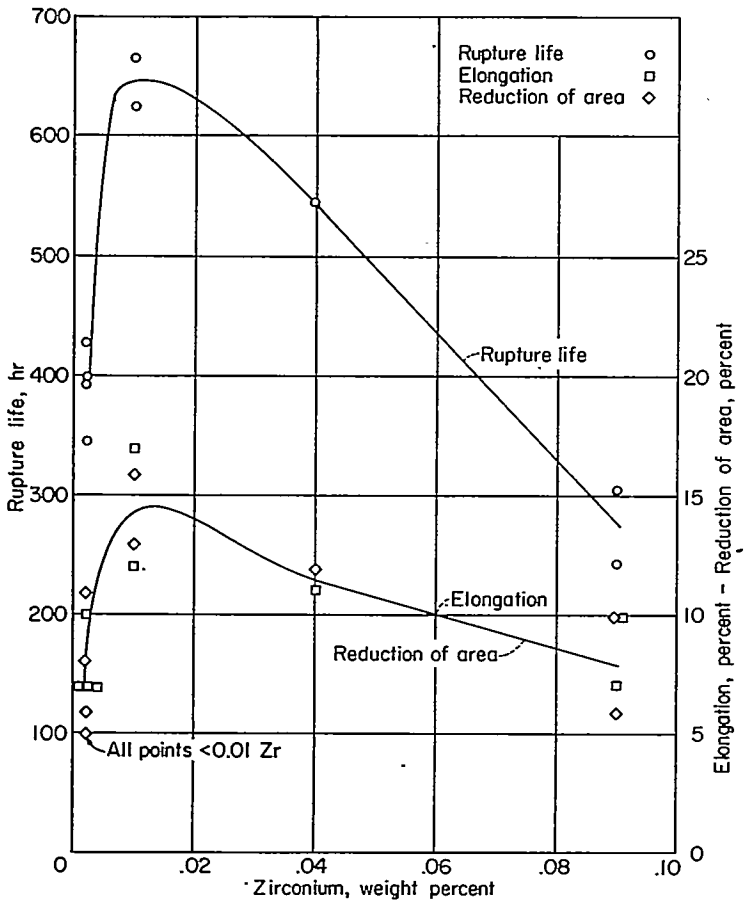

FIGURE 10.—Effect of zirconium content on rupture life and ductility at 1,600° F and 25,000 psi in presence of boron contents of 0.0069 to 0.0090 percent.

made (heat V–14) with 0.0088 percent boron and 0.01 percent zirconium was slightly stronger than the commercial material.

In connection with the mechanism studies a few rupture tests were conducted at stresses other than 25,000 psi. The data obtained are given in table V and the points are shown graphically in figure 11. While the data are too sparse to permit drawing curves of stress against rupture time, there is a suggestion of steeper curves in two cases than is typical for the curves for Udimet 500.

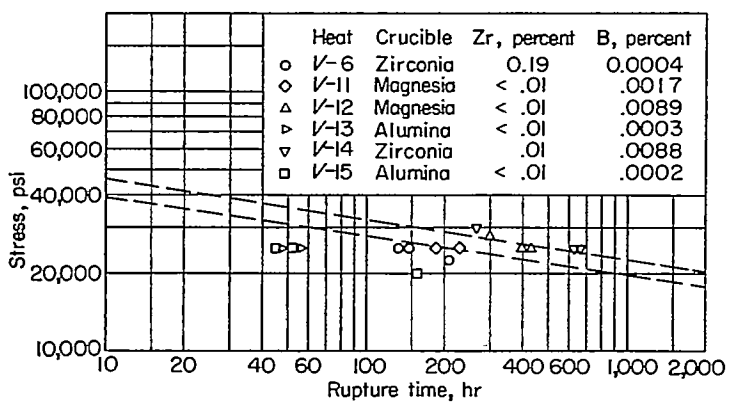

FIGURE 11.—Effect of stress on rupture life at 1,600° F. Data plotted as dashed rupture band were from two heats of commercial Udimet 500 alloy as reported by Utica Drop Forge and Tool Div. of Kelsey-Hayes Co. Heat treatment for commercial alloy was 2 hours at 2,150° F, air-cooled, plus 4 hours at 1,975° F, air-cooled, plus 24 hours at 1,550° F, air-cooled plus 16 hours at 1,400° F, air-cooled.

Creep characteristics: Typical creep curves from the rupture tests at 1,600° F at stresses of 25,000 and 20,000 psi are shown in figure 12. These curves are limited to material melted in alumina (heat V–15) with low boron and zirconium, heat V–6 with 0.19 percent zirconium resulting from reaction with the zirconia crucible, heat V–12 with 0.0089 percent boron, and heat V–14 with 0.0088 percent boron and 0.01 percent zirconium. Other heats had intermediate curves in accordance with their rupture strengths.

The effect of boron and zirconium on creep characteristics for the conditions considered can be summarized as follows:

(1) Neither boron nor zirconium had much effect on primary creep.

(2) Secondary creep rates decreased (i. e., creep strength increased) with zirconium. Boron reduced creep rates still more and boron plus zirconium in the amounts in heat V–14 resulted in the lowest second-stage creep rates (see fig. 13). In fact, the boron heat and the boron-plus-zirconium heat decreased in length during tests at 20,000 psi (fig. 12 (b)). Boron also prolonged second-stage creep (fig. 12 (a)).

(3) Both zirconium and boron prolonged third-stage creep and increased the amount of third-stage creep before fracture occurred (fig. 12 (a)). The amount of boron plus zirconium in heat V–14 was most effective in this respect.

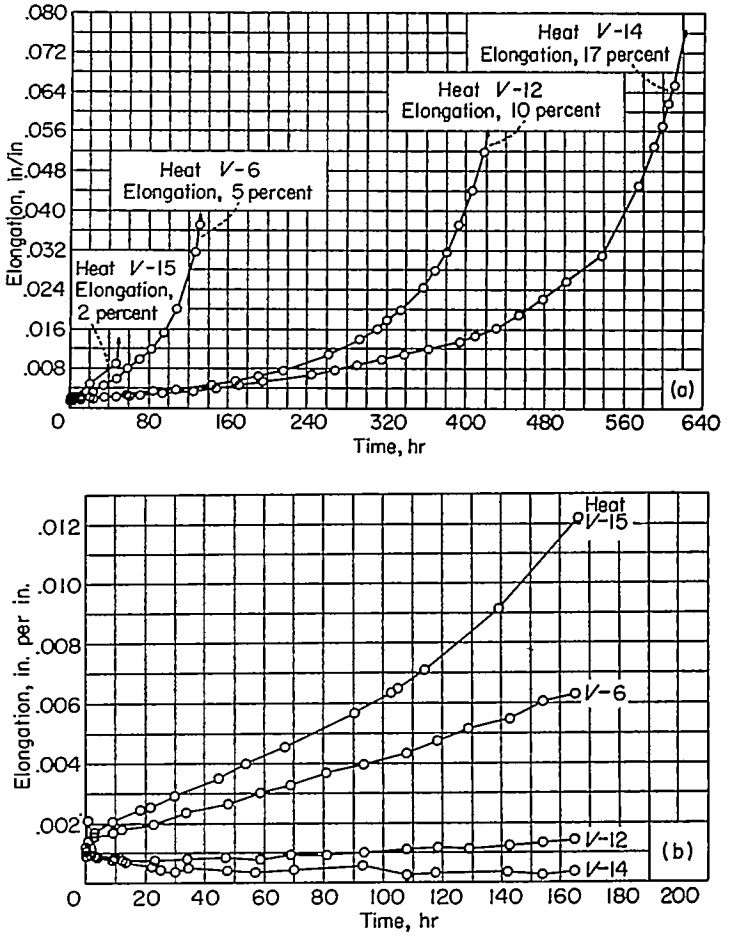

(a) Stress, 25,000 psi.
(b) Stress, 20,000 psi.

FIGURE 12.—Comparative creep curves at 1,600° F.

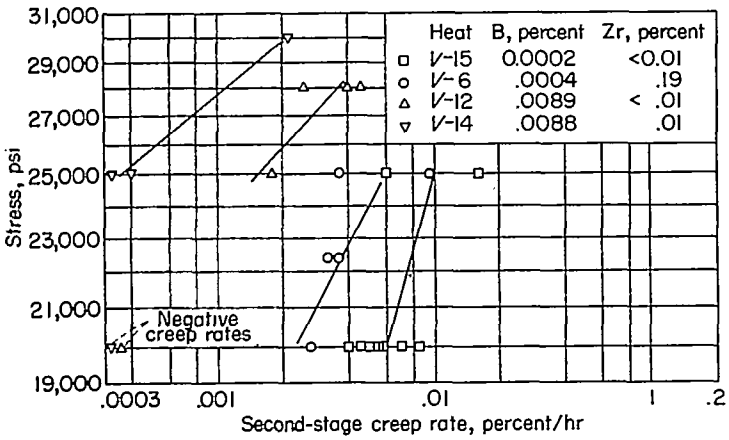

FIGURE 13.—Influence of stress on second-stage creep rate at 1,600° F.

Discussion.—The properties of the experimental alloy were influenced to a marked extent by the type of ceramic used for induction melting in vacuum. The chemical analyses indicate that, if boron or zirconium were not introduced into the melt by reaction with the crucible, rather inferior properties resulted. There seems to be little doubt that the effects of the reaction with crucibles can be a major factor in the variation in strength and ductility at high temperatures and in hot-workability of vacuum-melted heat-resistant alloys containing titanium and aluminum.

Most commercial induction vacuum melting uses magnesia or high-magnesia-content refractories for crucibles. Variation in the amount of reaction with the crucible could be, and probably is, a source of variable properties. Less effect in the second than in the first heat from a magnesia crucible suggests that the effect varies between successive heats from one crucible. The use of patching between heats and other possibilities of erratically providing fresh ceramic surfaces with increased reactivity to melts could be involved. Consideration of the possibility of other sources of boron compounds, such as ceramic binders, should be recognized.

Boron compounds are usually associated with magnesia as a contaminant; therefore, the derivation of boron from the crucible appears to be readily explainable. However, it is probable that recoveries of boron vary with a number of factors including the temperature and time of contact of the melt with the crucible, the ratio of crucible surface to melt volume, the number of heats, the variation in boron content of the magnesia crucible, and probably the compositional variations of the alloy.

The stability of the crucible materials may differ with melting atmosphere and pressure. Although considerable melt-crucible reaction occurred in vacuum melting, such crucible reactions may be limited in air melting by the higher pressure and the presence of slag and skull on the crucible walls.

The results also serve to suggest that the inadvertent introduction of even minute amounts of boron with the charge could be responsible for considerable variation in properties. The chances are that this occurs frequently, even though it may be unrecognized.

The data indicate that there are optimum amounts of boron when other trace elements, such as zirconium, are present. It seems probable that this has operated to give confusing results when elements such as boron and zirconium were knowingly or unknowingly added to heats simultaneously. There is a good chance that alloying elements other than boron and zirconium which are not yet recognized could exert a profound effect.

The relationship of the analyzed boron and zirconium contents to properties should not be accepted as complete establishment of compositional effects without further proof. There may be efficiency effects depending on their reaction with other elements not present in the heats studied so that total boron or zirconium content may not be directly related to properties. Furthermore, there is a possibility that heat and ingot size along with hot-working conditions were influencing results. It is also important to realize that analysis methods for boron and zirconium are subject to variation and that different laboratories might differ in the amounts reported.

The rupture tests were carried out on material heat-treated at 2,150° F and air-cooled. This differs from the usual heat treatment of 4 hours at 1,975° F plus 24 hours at 1,550° F plus 16 hours at 1,400° F. Other research in progress indicates that the treatment at 2,150° F minimizes variation in properties due to the influence of hot-working conditions. In particular, it appears to prevent abnormally low strength sometimes encountered when a 1,975° F treatment is applied to as-hot-worked material. A subsequent treatment at 1,975° F after a 2,150° F treatment usually gives the same properties as a single treatment at 2,150° F. Very little difference in rupture strength and ductility has been observed for inclusion or omission of the aging treatments. Possibly the 4 hours used to equalize temperatures before testing cause the inclusion or omission of prior aging to have little influence. All experiences to date indicate the test results reported for a simple solution treatment at 2,150° F to be generally characteristic of the alloy when treated at 1,975° F except for the elimination of occasional low strength values.

Carbon content of the alloys varied more than was desired. The major reason for the variability of carbon content was the wide range of melting conditions employed with the consequent difficulty of controlling carbon recovery. This may be an additional factor in the variation of properties.

The data on the influence of titanium and aluminum content are not so complete as would be desirable. More variation than was intended occurred in the heats. As noted previously, there apparently was longer rupture life with a given zirconium content when titanium-plus-aluminum content was high. This probably resulted from the higher titanium-plus-aluminum level providing a larger percent by volume of $Ni_3(Al,Ti)$ during stress-rupture testing.

The relationships between crucible ceramics and properties were developed for induction vacuum melting. The amount of such effects under other conditions of melting is not clear at this point. It is interesting to note that the ductility in rupture tests was low when the alloy was made in alumina crucibles. Low-zirconium heats made in zirconia crucibles and a low boron heat made in magnesia also had low ductility. This suggests that a part of the usual increase in ductility attributed to vacuum melting may be due to the opportunity

offered by vacuum melting to introduce effective trace elements from crucibles. Also, addition of trace elements other than boron and zirconium by other melting procedures may alter the effectiveness of a given boron and zirconium level.

The crucible-reaction effects were discovered as a result of inability to define the effects of variable-melting practices and the role of oxygen and nitrogen, the original objectives of the investigation. The crucible reactions must be controlled before the influence of the melting variables can be defined. Because of the sensitivity of properties to reactions with magnesia along with interrelated effects from such factors as hot-workability, very careful research will be necessary to define the effects clearly. While the data of this report suggest that many melting variables are secondary to the introduction of boron or zirconium from the crucibles, there may be extenuating circumstances which mask the effects. The subject is of sufficient complexity that probably the only way it can be cleared is by clarification of the mechanism by which as little as 15 parts per million of boron can increase rupture life 5 times.

In spite of the limitations on the generality of the results it is believed that the data reported reflect production experience quite well. Many of the variations in properties in the experimental investigation and in commercially produced alloys of the type investigated seem to be explainable in terms of the results of the investigation.

MECHANISM OF BENEFICIAL EFFECTS OF BORON AND ZIRCONIUM

Marked differences in microstructures after exposure to creep at 1,600° F were found in the four heats which showed extremes in properties as a function of boron and zirconium. In terms of properties, the most significant effects were found at those grain boundaries approximately normal to the applied stress during creep. In the low-boron-and-zirconium heat V–15, a process of agglomeration of $M_{23}C_6$ type carbide was accompanied by depletion of the γ' precipitate from the adjacent matrix and finally microcracking leading to early brittle fracture. This process was found to be retarded by the zirconium in heat V–6. Boron in heat V–12 retarded the process even more while the boron plus zirconium in heat V–14 was most effective. This increasingly effective retardation of eventual microcracking appeared to be mainly responsible for improved properties. Other less effective structural differences were observed between the heats.

Few, if any, significant differences in microstructure as a function of composition were present in specimens aged at 1,600° F without stress. Specimens which were fractured in rupture tests also showed few significant differences. The structures of specimens after varying amounts of creep provided the most useful information. The exposure conditions for the specimens of the four heats studied are summarized in table V. The conditions of exposure were selected to show structures after rupture under 25,000 psi and after varying amounts of creep under 20,000 psi. Stresses were also adjusted so that a series of specimens representative of all four heats could be examined after undergoing approximately the same amount of creep in the same time periods.

The microstructural features were found to be best expressed on a "quantitative" basis. Accordingly, the observations for the samples aged under stress are summarized in table VI and for those aged without stress, in table VII. The significant features are discussed in the following sections.

Microstructures in initial condition.—After the initial homogenizing treatment of 2 hours at 2,150° F and air-cooling the experimental heats were similar in grain size, inclusion count, and distribution (figs. 14 (a) to 14 (d)), and in grain-boundary precipitate (figs. 14 and 15). During the air-cooling after the 2,150° F treatment γ' precipitated. Some slight differences in dispersion of intragranular γ' existed but these were not found to be significant (as discussed later). Hardnesses (figs. 14 (a) to 14 (d)) did not differ significantly in this condition.

Agglomeration in grain boundaries.—A network of carbides enveloped by γ' accumulated in the grain boundaries of all samples during exposure at 1,600° F. In heat V–15 the rate of accumulation was comparatively rapid, the carbide phase being extensive and blocky and the γ' layer thick after 165-hour exposure with 1.2-percent creep deformation (figs. 16 and 17). The amount of agglomeration under these conditions was somewhat lower in the presence of zirconium (heat V–6) and much lower when boron (heat V–12) or boron plus zirconium (heat V–14) were present (figs. 16 (e) to 16 (h) and 17).

The agglomerated γ' was easily identified by etching characteristics. The agglomerate reacted to etching in the same manner as did the intragranular γ' in all the experimental work carried out. It always was in the same relief and had the same appearance as did the intragranular γ'.

Microfractographic techniques were used to identify the carbide phase and obtain more information on its form. Samples from heats V–15 and V–12 after 1.2-percent creep deformation at 1,600° F in 165 to 188 hours were cooled in liquid nitrogen and then fractured. Extraction replication from the fractured surface removed the grain-boundary carbide and retained it in the replica. Electron micrographs showing the size and distribution of carbides in the grain boundaries are shown in figure 18. The extracted particles from the heat free from boron or zirconium (V–15) were larger, more extensive and thicker than those from the heat with boron (V–12). The electron diffraction spots obtained on the replicas of the two samples indexed for $M_{23}C_6$.

Depletion of γ' at grain boundary.—Subsequent to the agglomeration of $M_{23}C_6$ in the grain boundaries, strips of matrix were depleted of γ' particles along transverse grain boundaries of the specimens aged under stress (fig. 19). This occurred most often adjacent to $M_{23}C_6$ particles. This was in contrast with samples aged without stress, where the

intergranular $M_{23}C_6$ was always enveloped by γ' and where the fine γ' particles extended up to the grain boundary (figs. 20 and 21).

In figure 19 the amount of this depletion is related to creep deformation for the experimental heats exposed to give equal strain at equal time at 1,600° F. It is evident that boron and zirconium are effective in reducing the amount of this depletion with a given strain at 1,600° F. Since the samples were stressed to give comparable strain rates, it follows that depletion in a given time at 1,600° F was reduced. Despite this retarding influence, however, the amounts of depletion at fracture became comparable in

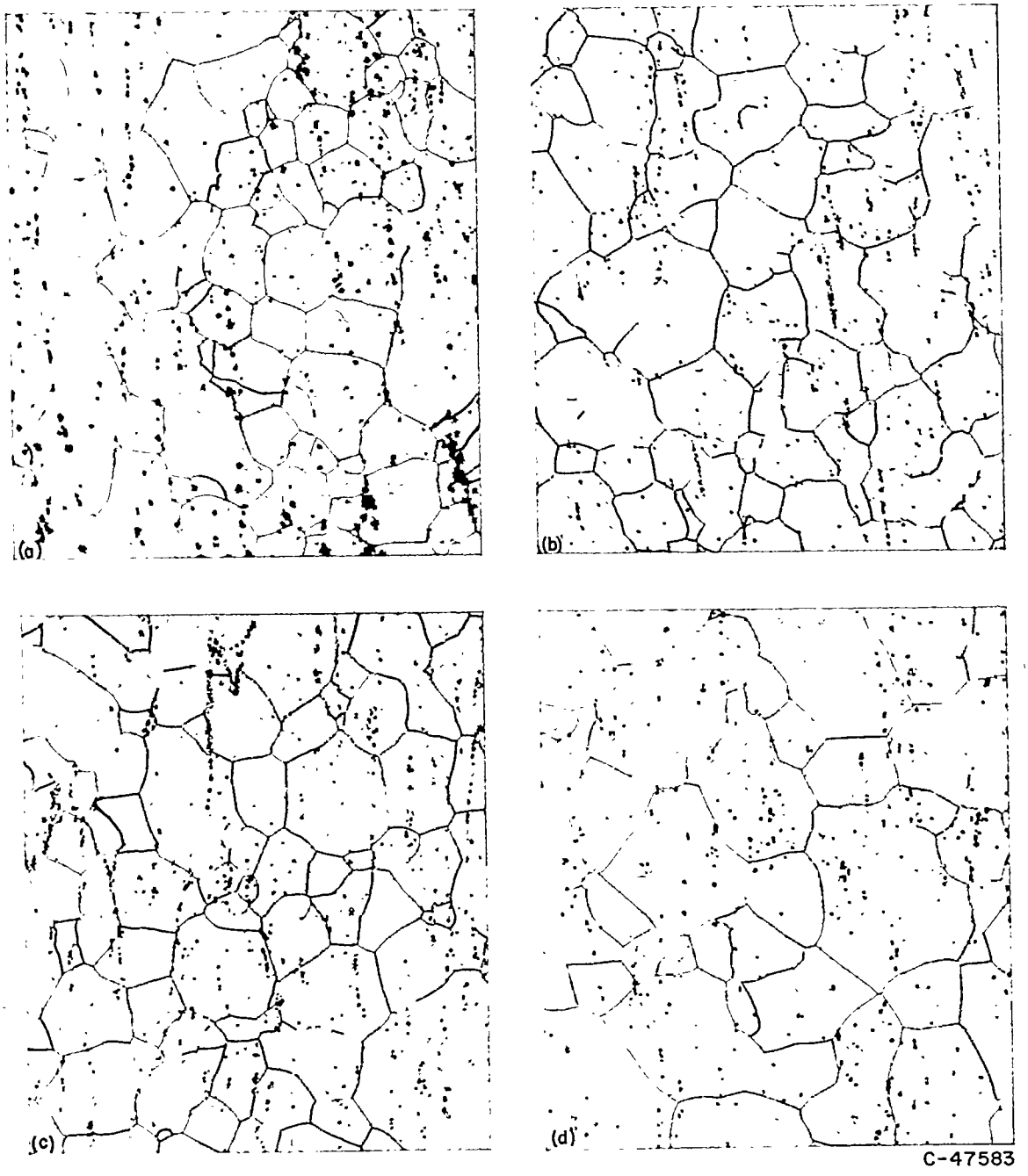

(a) Heat V–15; diamond pyramid hardness, 354; X100.
(b) Heat V–6; diamond pyramid hardness, 353; X100.
(c) Heat V–12; diamond pyramid hardness, 345; X100.
(d) Heat V–14; diamond pyramid hardness, 348; X100.

FIGURE 14.—Microstructures of specimens treated 2 hours at 2,150° F, then air-cooled. Optical micrographs; X100 and X1,000.

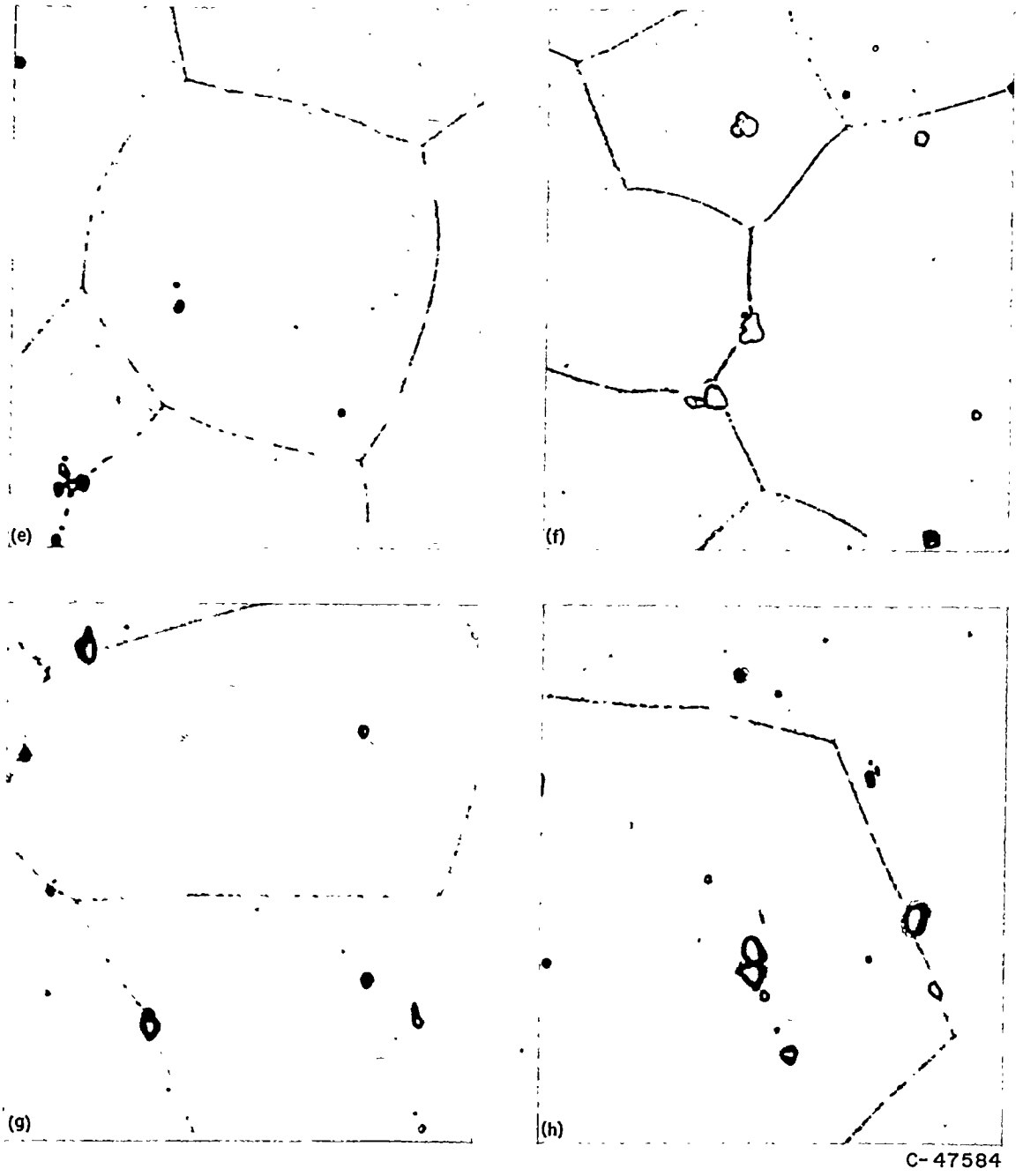

(e) Heat V–15; X1,000.
(f) Heat V–6; X1,000.
(g) Heat V–12; X1,000.
(h) Heat V–14; X1,000.

FIGURE 14.—Concluded.

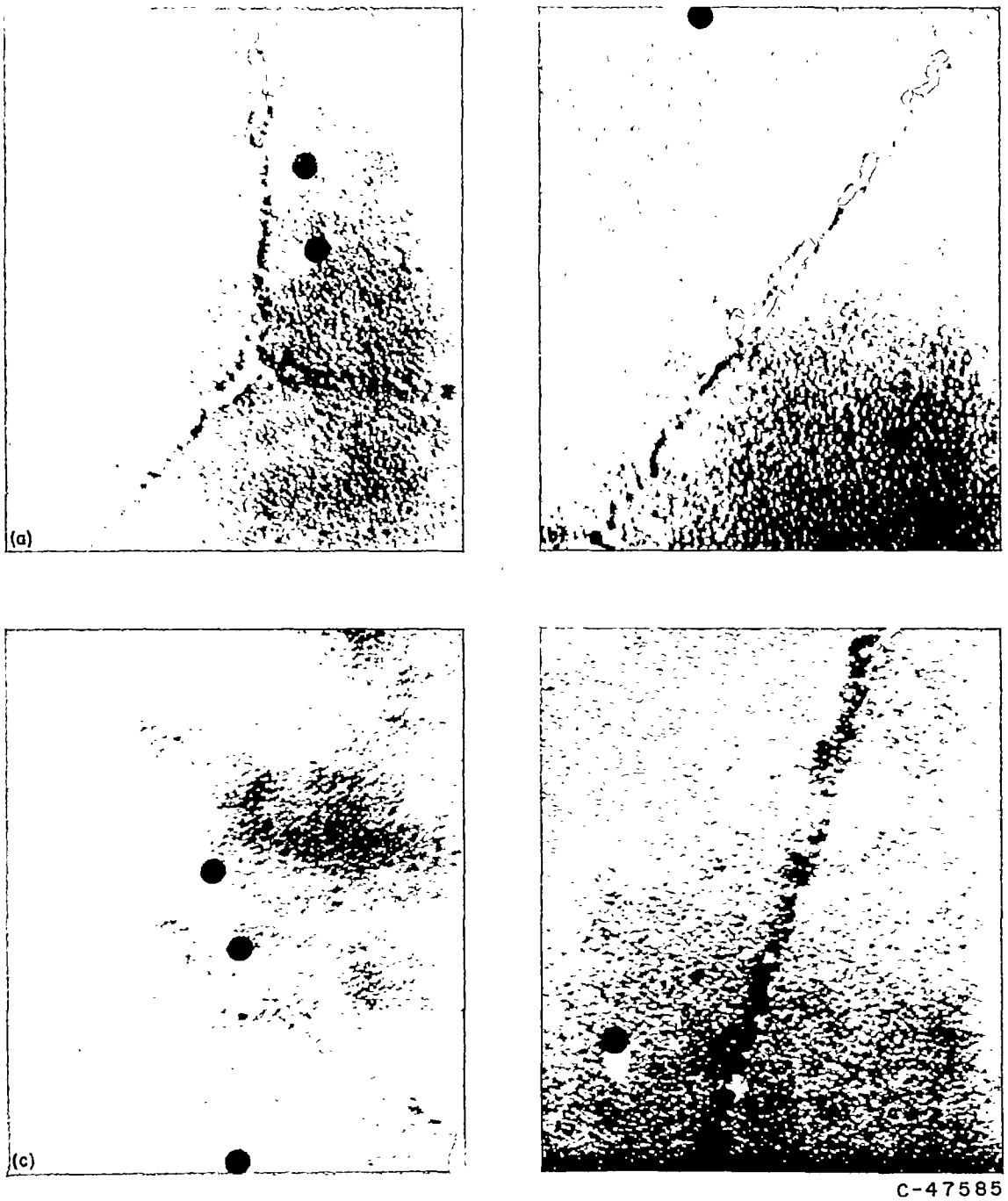

(a) Heat V–15.
(b) Heat V–6.
(c) Heat V–12.
(d) Heat V–14.

FIGURE 15.—Microstructures of specimens treated 2 hours at 2,150° F, then air-cooled. Electron micrographs; X12,000.

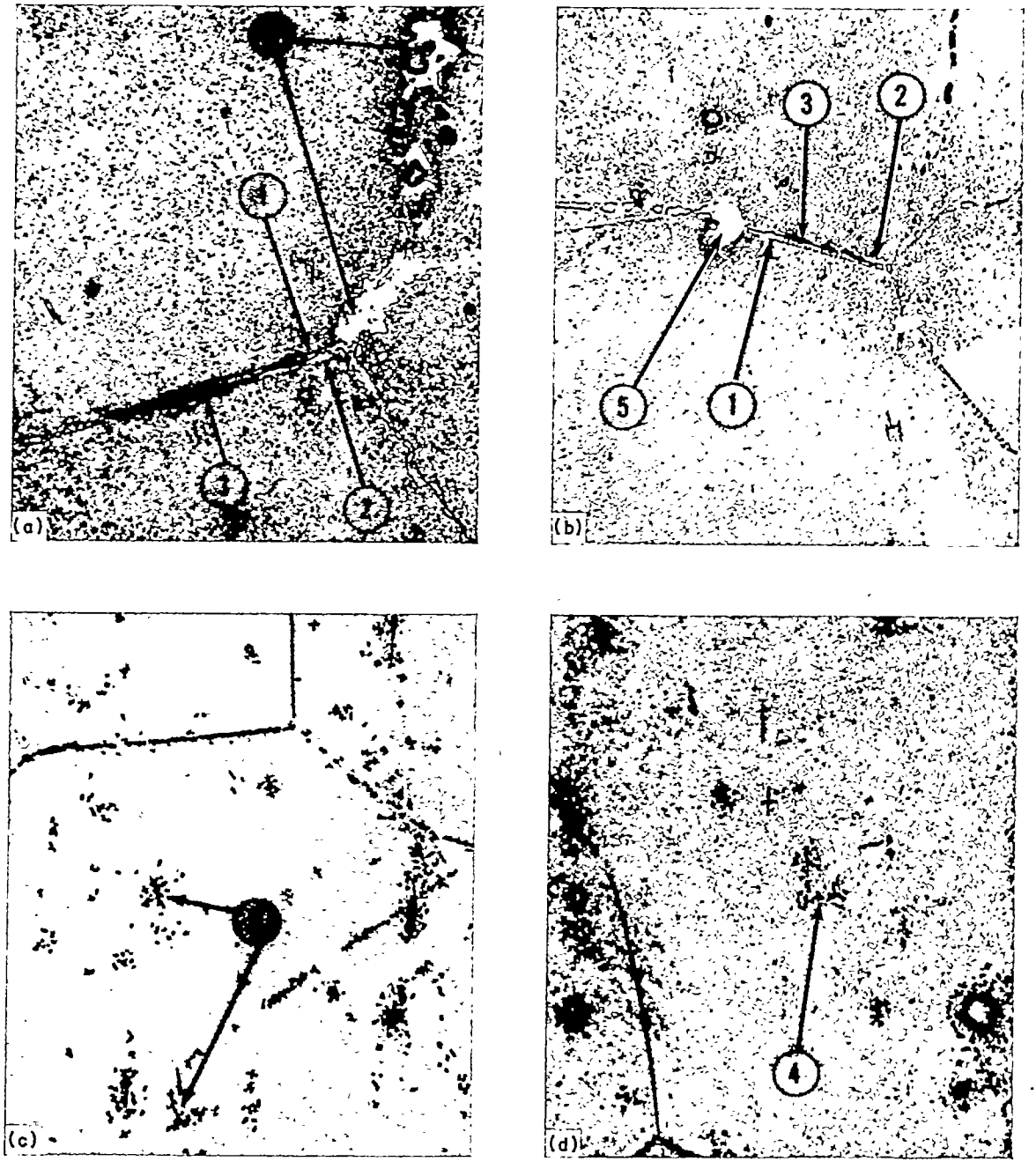

(a) Heat V–15; X1,000.
(b) Heat V–6; X1,000.
(c) Heat V–12; X1,000.
(d) Heat V–14; X1,000.

FIGURE 16.—Microstructures of specimens after 1.2-percent deformation by creep at 1,600° F in 165 to 214 hours. Optical micrographs; X100 and X1,000. 1, intergranular $M_{23}C_6$; 2, depleted grain boundary; 3, microcrack; 4, intragranular carbide; 5, nodule.

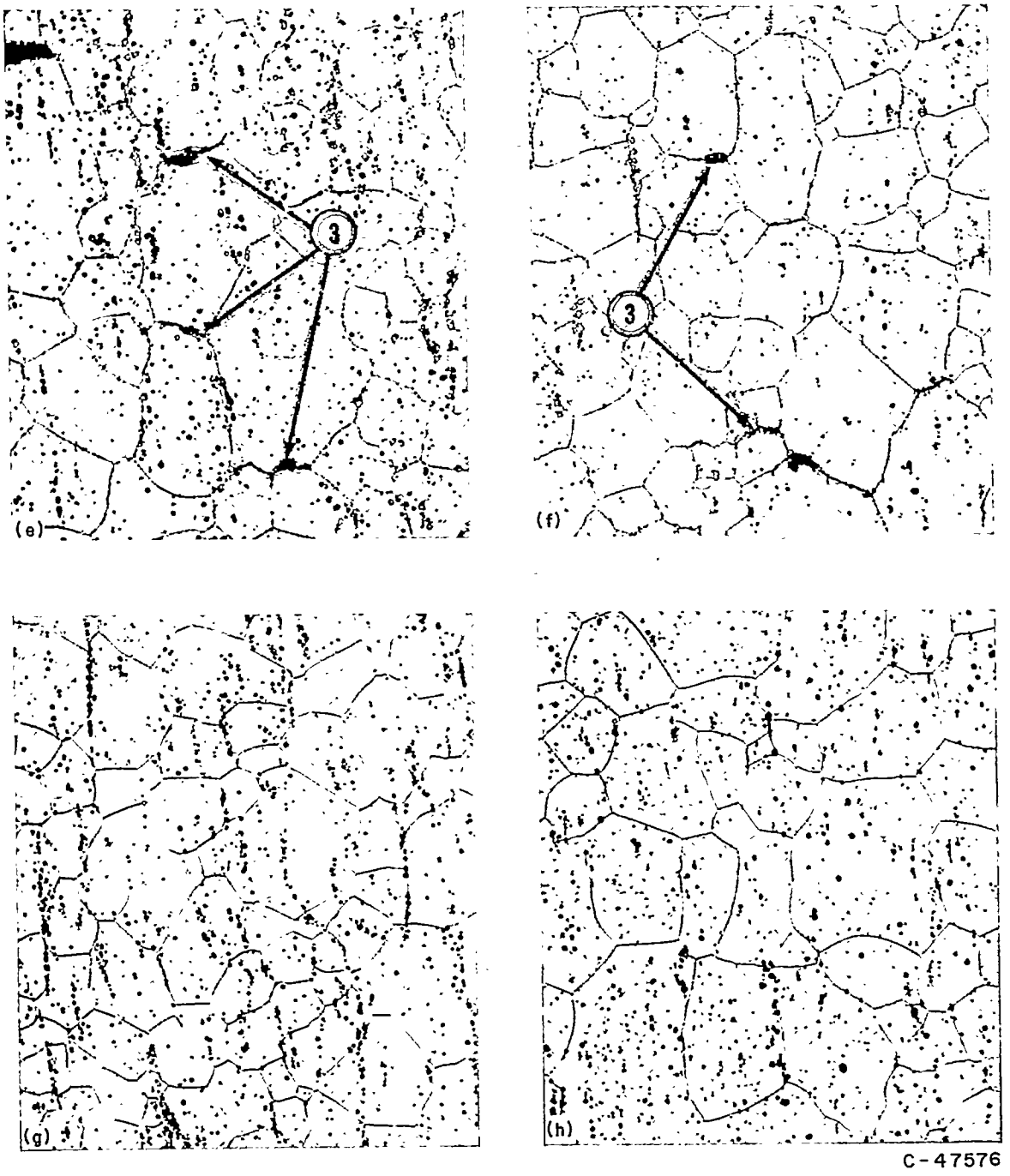

(e) Heat V–15; electropolished; X100.
(f) Heat V–6; electropolished; X100.
(g) Heat V–12; electropolished; X100.
(h) Heat V–14; electropolished; X100.

FIGURE 16.—Concluded.

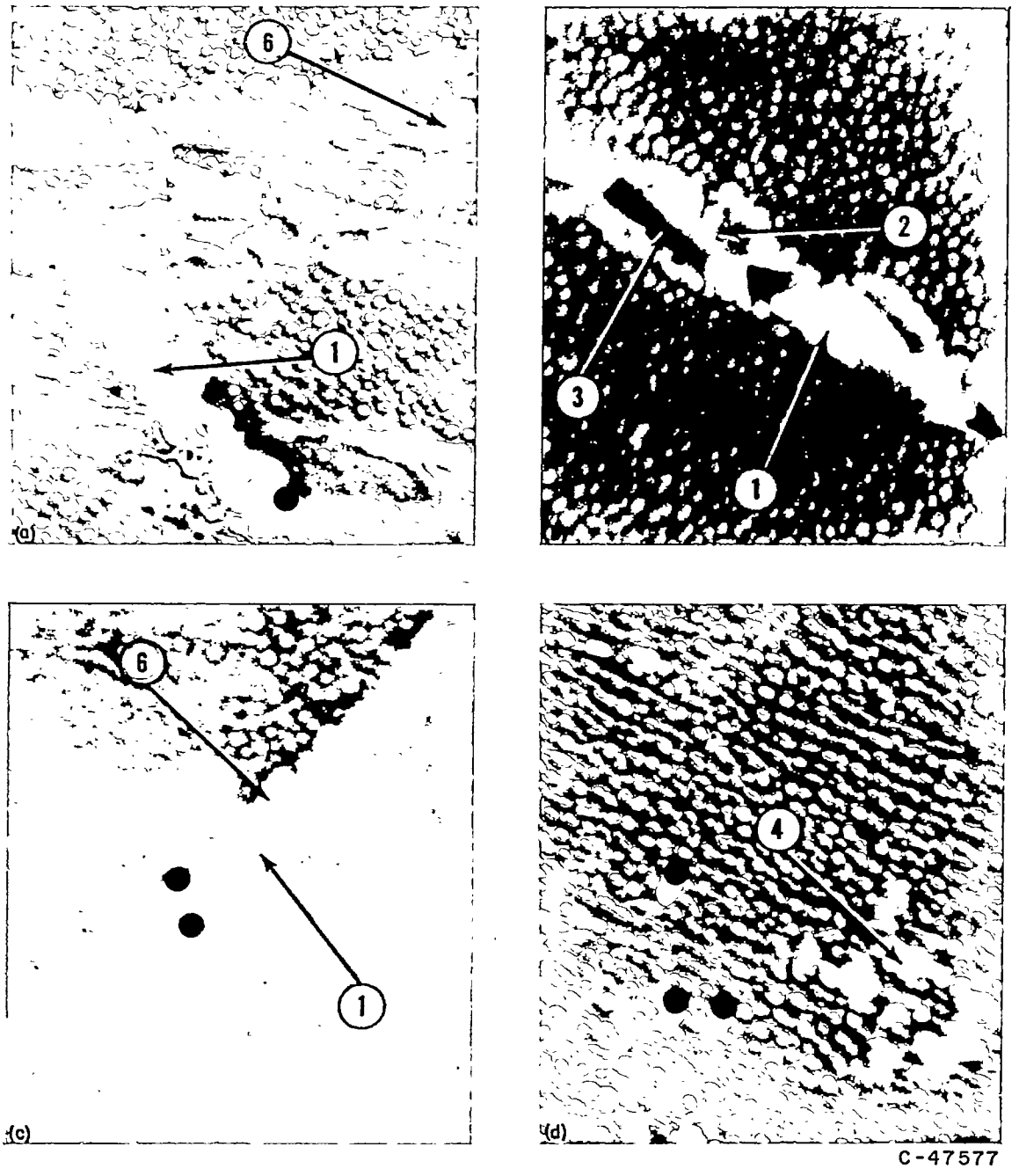

(a) Heat V–15; typical grain boundaries.
(b) Heat V–6; depleted and cracked grain boundary at typical $M_{23}C_6$ precipitate.
(c) Heat V–12; typical grain boundary.
(d) Heat V–12; intragranular carbides and alinement of γ'.

FIGURE 17.—Microstructures of specimens after 1.2-percent deformation by creep at 1,600° F in 165 to 214 hours. Electron micrographs; X12,000. 1, intergranular $M_{23}C_6$; 2, depleted grain boundary; 3, microcrack; 4, intragranular carbide; 6, γ'; 7, Ti(C,N).

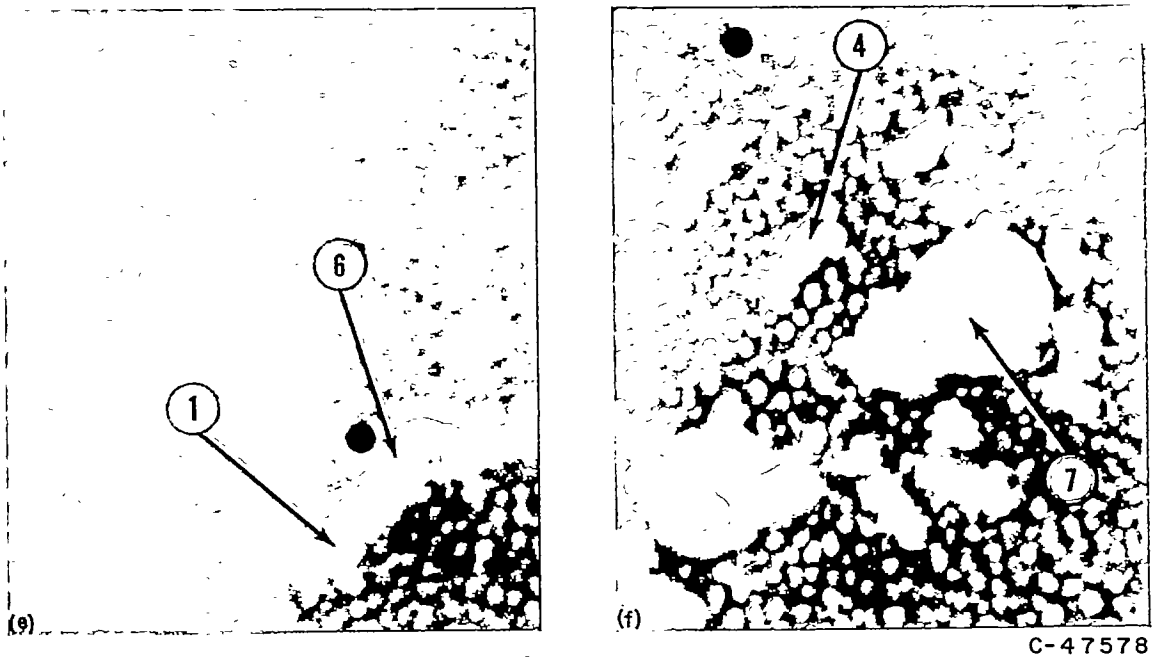

(e) Heat V–14; typical grain boundary and alinement of γ'.
(f) Heat V–14; intragranular carbides surrounding Ti(C,N).

FIGURE 17.—Concluded.

the heats with zirconium, boron, or boron plus zirconium. Presumably the increased strain to fracture was responsible.

In samples ruptured at 1,600° F and 25,000 psi (fig. 22) the depletion was extensive. Often, layers of precipitate-free matrix as thick as 5 to 10 microns were found. In this case comparison of retardation was limited by the unequal exposure times and strains, although the effectiveness of zirconium, boron, and boron plus zirconium was very evident.

After 165 hours at 1,600° F at an equal stress of 20,000 psi, the retarding effect of boron and zirconium was even more evident. While 264 depleted boundaries were found in heat V–15, only 72 were found in the heat V–6 with zirconium, 16 in heat V–12 with boron, and none in heat V–14 with boron plus zirconium (table VI).

Microcracks.—Following agglomeration of $M_{23}C_6$ and depletion of γ' in the grain boundaries, microcracks appeared. These appeared as dark areas in mechanically polished samples (figs. 16(a) to 16(d)). Confirming evidence of cracks was found in electron microscopy where the replicas contained fins where the collodion had filled microcracks and then had been extracted during stripping of the replica from the metal surface. The fins appeared black in the electron micrographs (fig. 17) with white shadows from palladium.

The microcracks were associated with $M_{23}C_6$ particles in the grain boundaries transverse or nearly transverse to the applied stress, usually being at an $M_{23}C_6$ matrix interface or between tips of $M_{23}C_6$ particles, in both cases where depletion of γ' had occurred. Often, several separate microcracks were detected in one grain boundary with no preference being shown for triple points. These separate cracks seemed to link together with further creep exposure, constituting the mode of fracture in heat V–15 (no boron or zirconium).

Figure 23 relates microcracking to creep deformation for exposure to equal strain in equal time at 1,600° F. The number of cracks for a given creep strain or exposure time diminished with zirconium (heat V–6), boron (heat V–12), and boron plus zirconium content (heat V–14) in that order from the boron-and-zirconium-free material (heat V–15). Five microcracks were detected in heat V–15 at the end of first-stage creep when only 15 percent of the rupture life was expended. When boron plus zirconium was present (heat V–14), only 2 microcracks were found at 80 percent of the rupture life when tertiary creep had already commenced. The amount of microcracking at fracture also diminished in the heats in the following order: heat V–15, heat V–6, heat

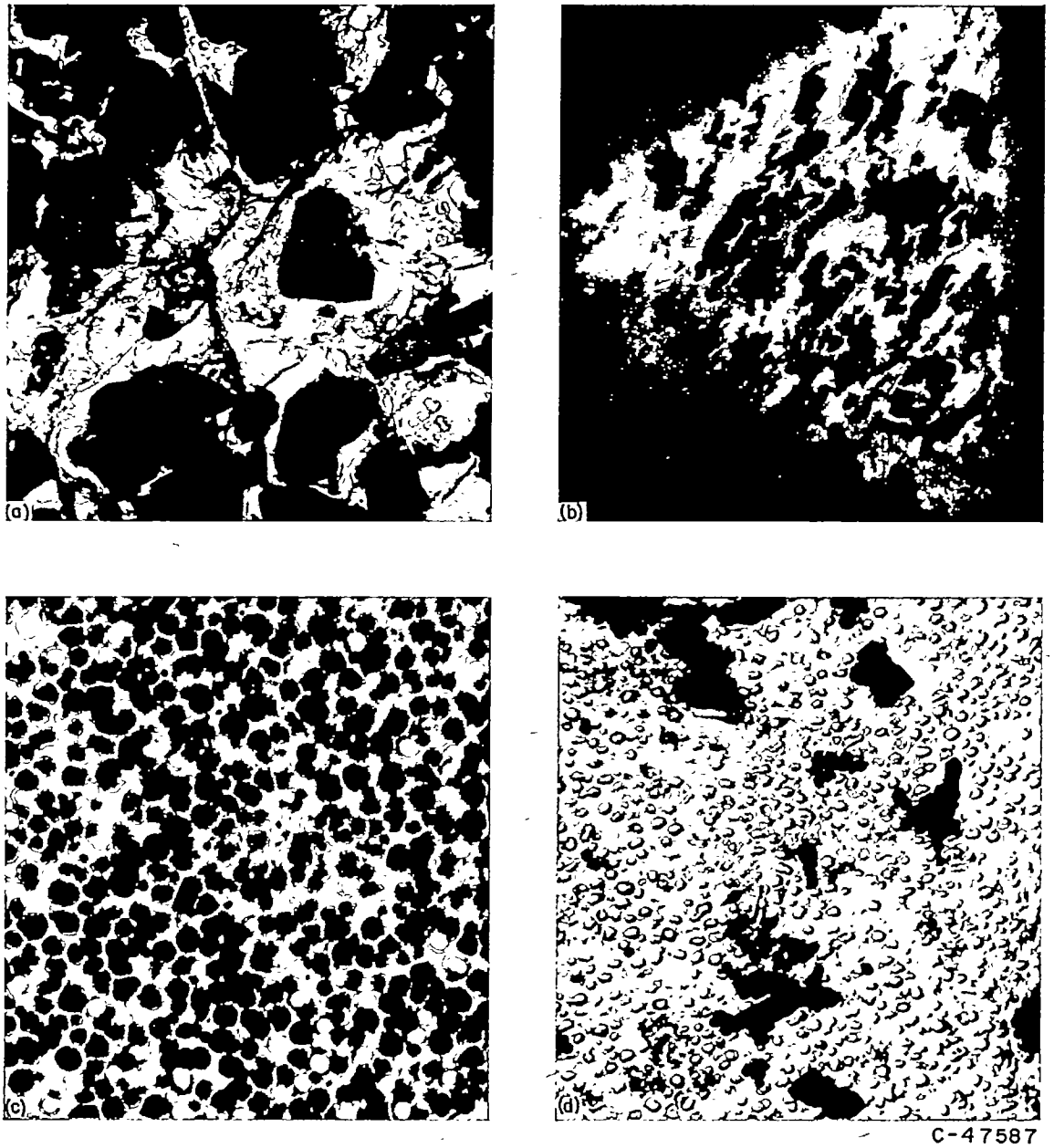

C-47587

(a) Extraction replica of carbide from intergranular fracture surface of heat V–15 after 1.2-percent creep deformation in 165 hours at 1,600° F. All selected-area electron-diffraction spots indexed as $M_{23}C_6$. X8,000.

(b) Extraction replica of carbide from intergranular fracture surface of heat V–12 after 1.2-percent creep deformation in 188 hours at 1,600° F. All selected-area electron-diffraction spots indexed as $M_{23}C_6$. X8,000.

(c) Extraction replica of intragranular γ' from heat V–6 after aging 10 hours at 1,600° F. All selected-area electron-diffraction spots indexed as γ'. X36,000.

(d) Extraction replica of intragranular carbide from heat V–12 after 1.2-percent creep deformation in 188 hours at 1,600° F. Most selected-area electron-diffraction spots indexed as M_6C; a few, as $M_{23}C_6$. X8,000.

FIGURE 18.—Electron micrographs of phases produced by extraction replica technique. Extracted particles of phases appear black.

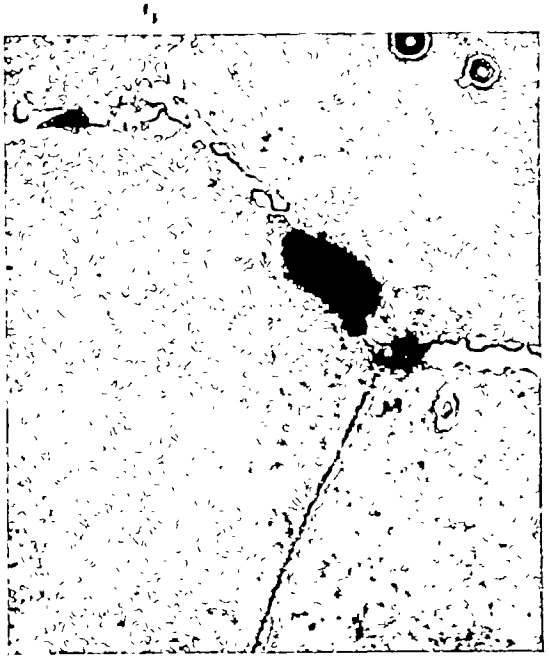

X2,000
Light micrograph

C-47588

X12,000
Electron micrograph

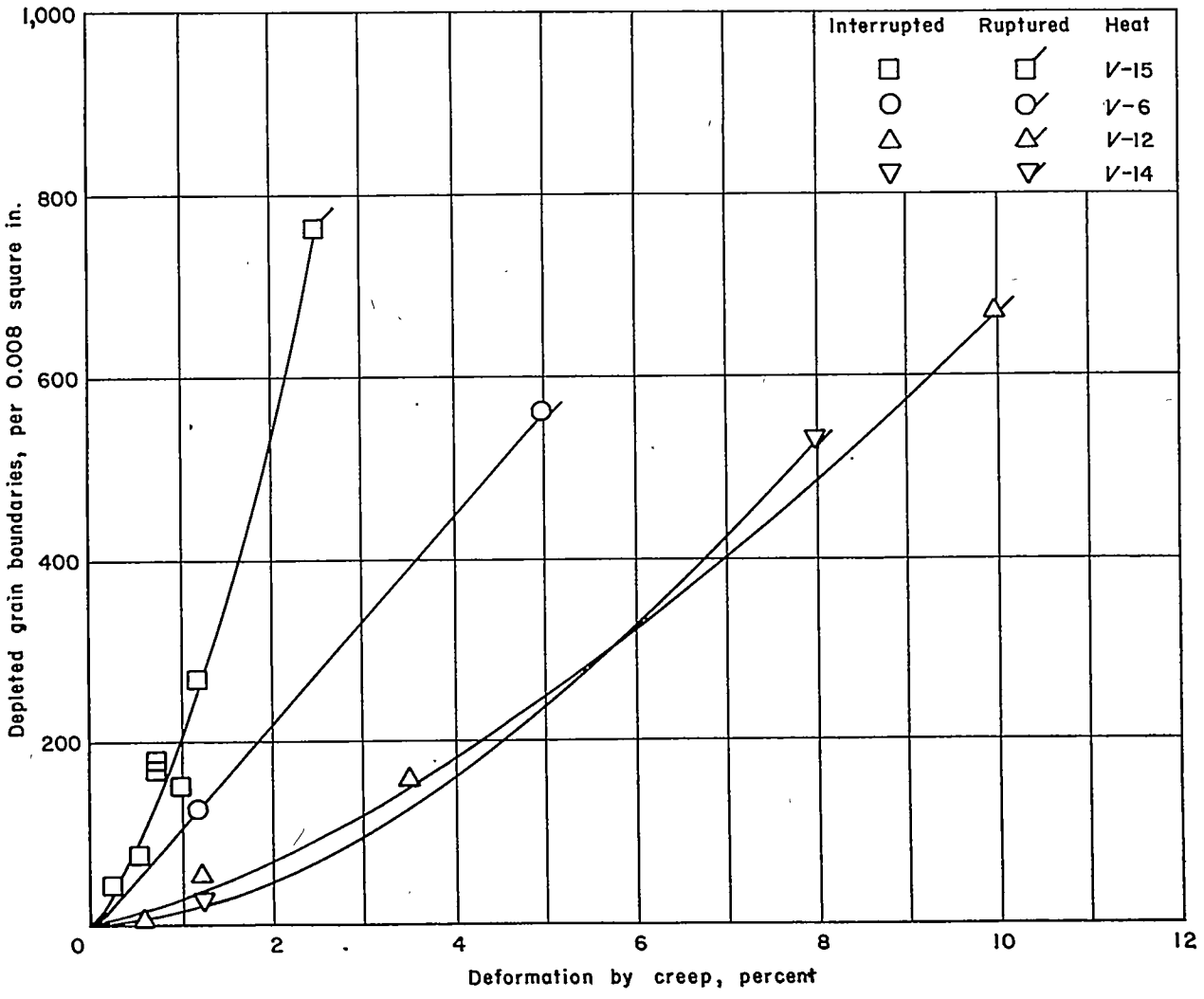

FIGURE 19.—Effect of creep deformation at 1,600° F on depletion of γ' adjacent to grain boundaries. Specimens were stressed to give comparable strain rates. Micrographs of typical depleted grain boundaries are shown for electropolished specimen.

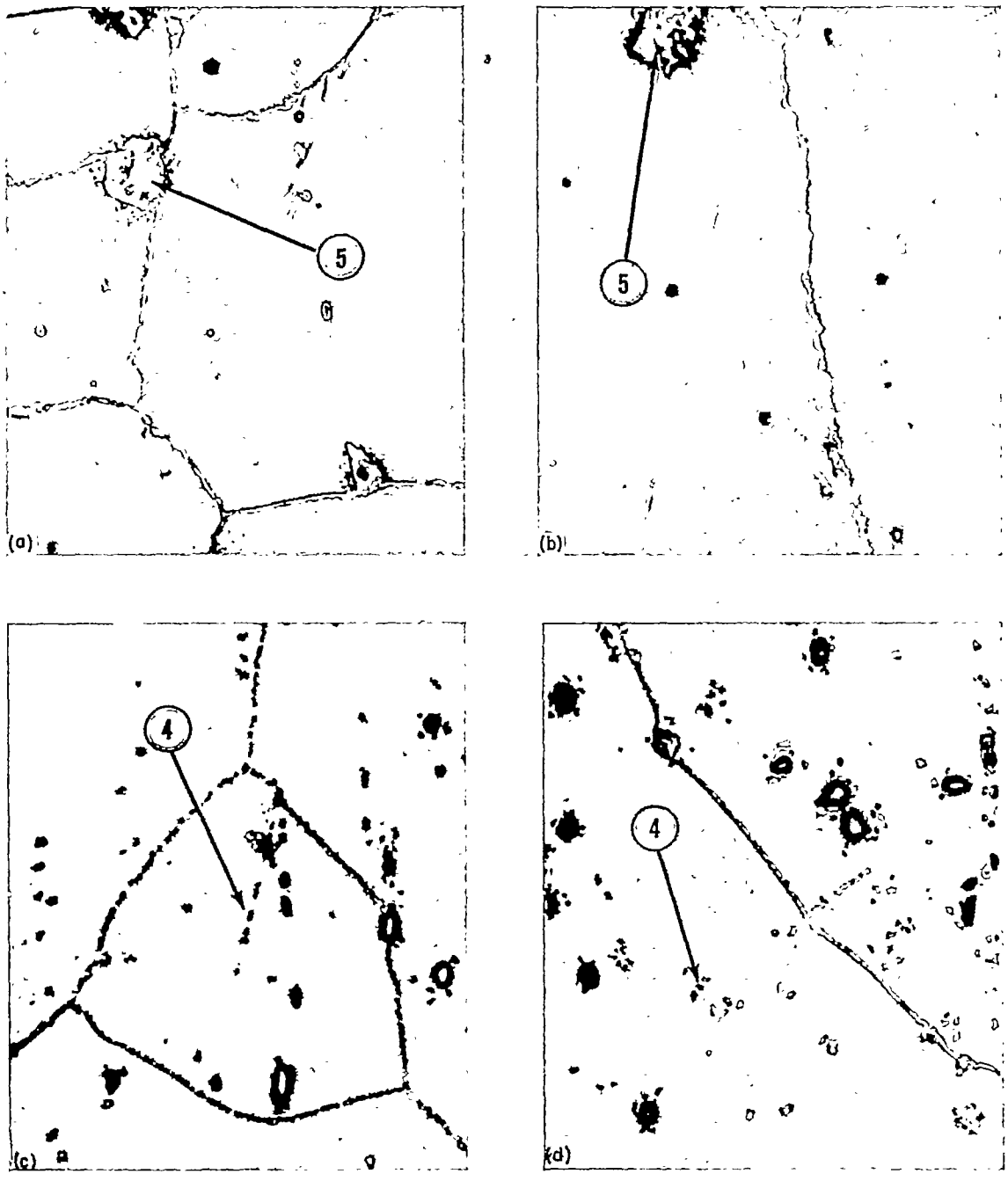

C-47579

(a) Heat V-15. Diamond pyramid hardness, 338.
(b) Heat V-6. Diamond pyramid hardness, 342.
(c) Heat V-12. Diamond pyramid hardness, 340.
(d) Heat V-14. Diamond pyramid hardness, 353.

FIGURE 20.—Microstructures of specimens after aging without stress for 188 hours at 1,600° F. Optical micrographs; X1,000. 4, intragranular carbide; 5, nodule.

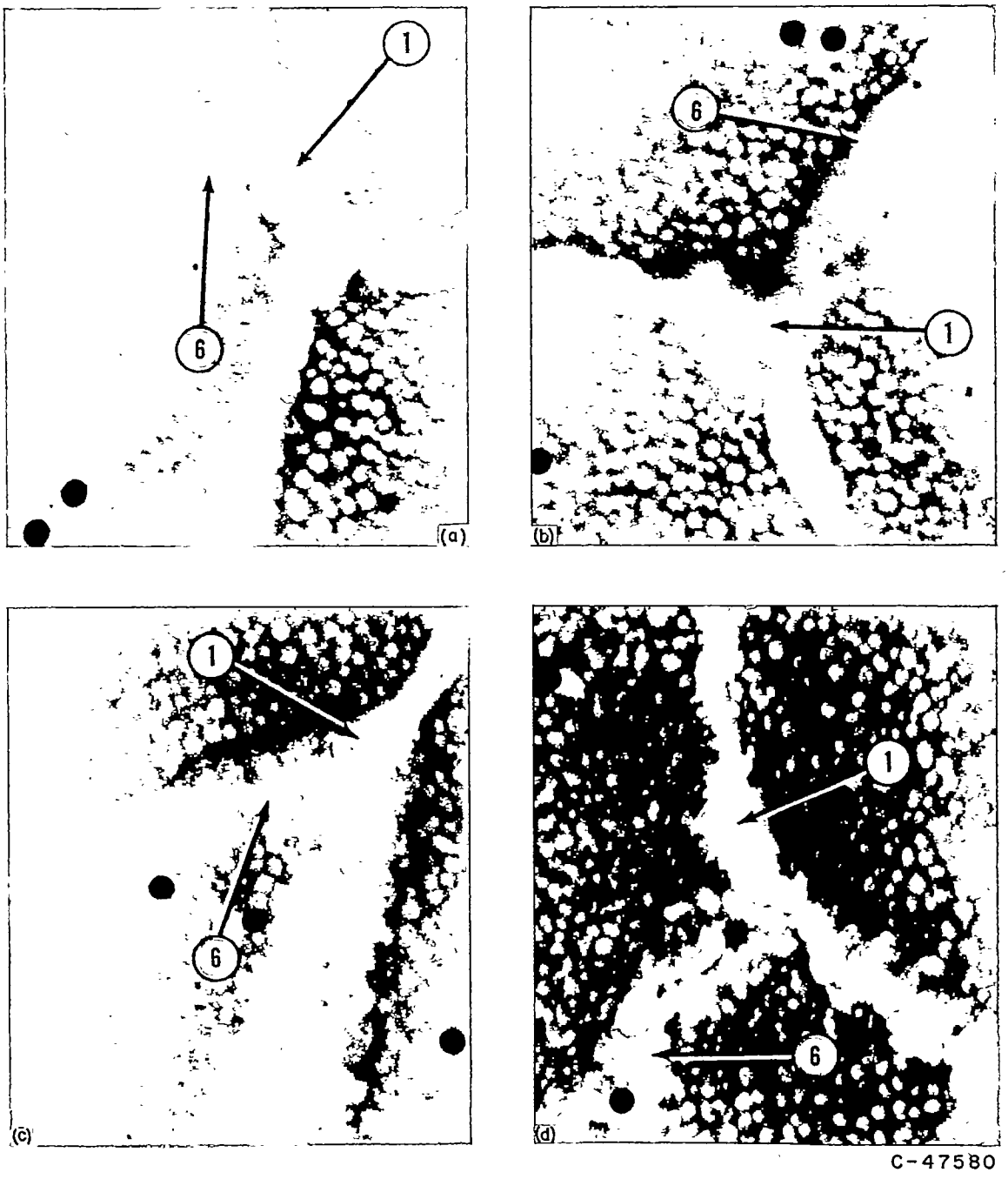

(a) Heat V–15.
(b) Heat V–6.
(c) Heat V–12.
(d) Heat V–14.

FIGURE 21.—Microstructures of specimens after aging without stress for 188 hours at 1,600° F. Electron micrographs; X12,000. 1, intergranular $M_{23}C_6$; 6, γ'.

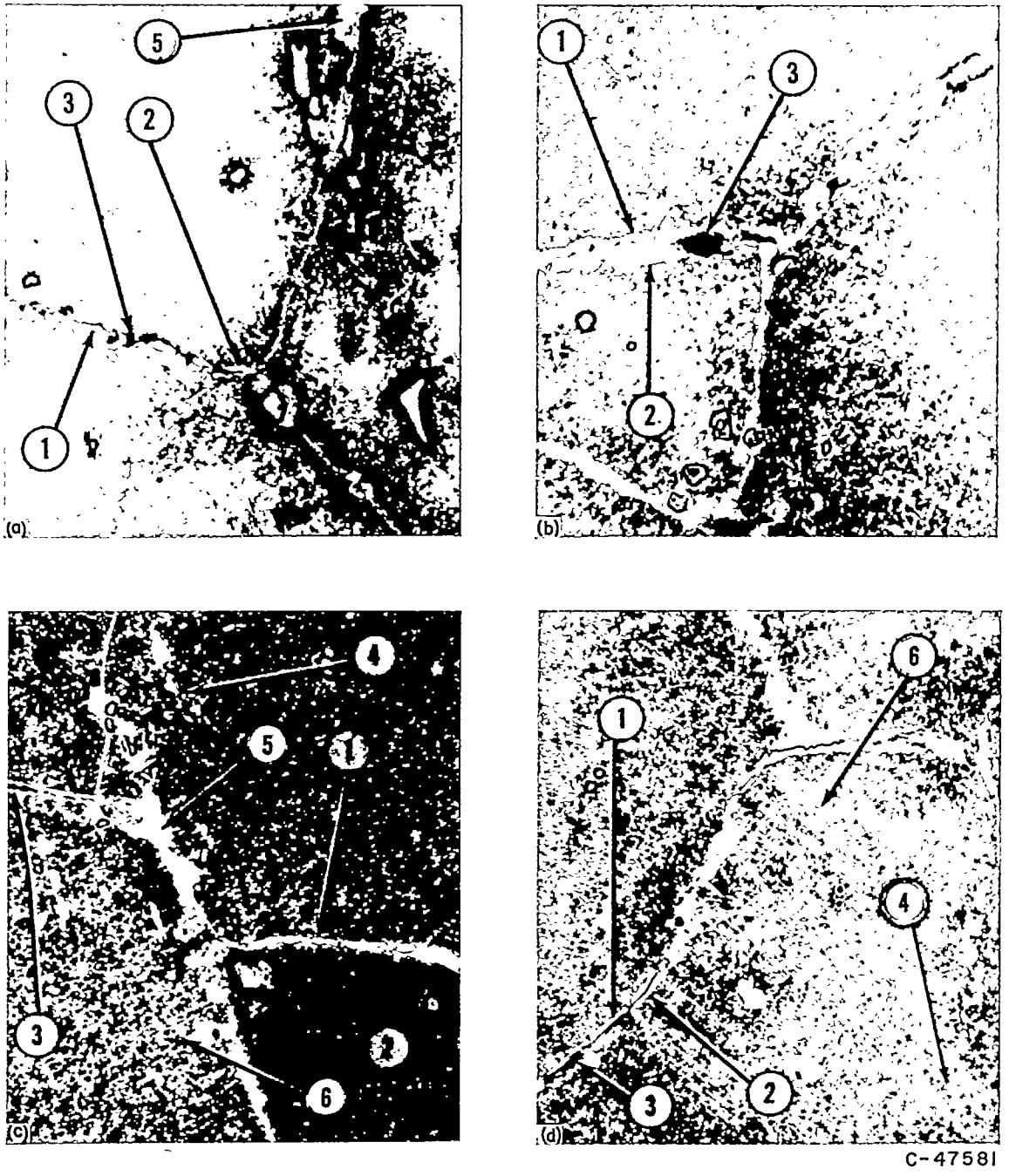

(a) Heat V–15.
(b) Heat V–6.
(c) Heat V–12.
(d) Heat V–14.

FIGURE 22.—Microstructures of specimens after rupture at 1,600° F and 25,000 psi. Optical micrographs; X1,000. 1, intergranular $M_{23}C_6$; 2, depleted grain boundary; 3, microcrack; 4, intragranular carbide; 5, nodule; 6, alinement of γ'.

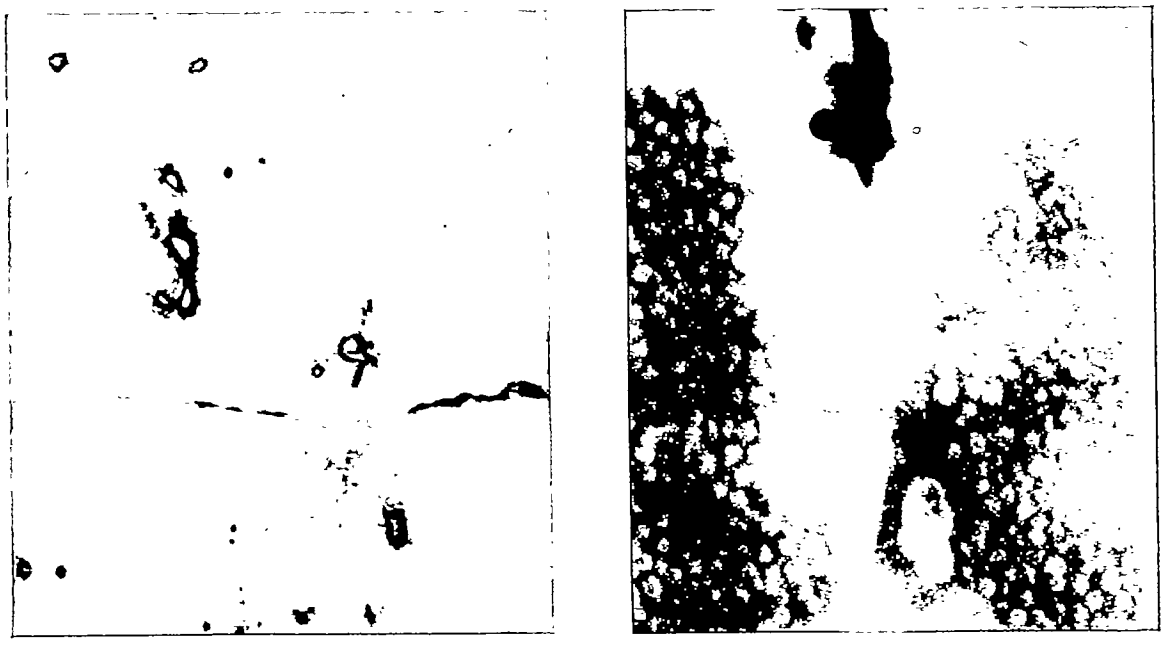

C-47589

X1,000
Light micrograph

X12,000
Electron micrograph

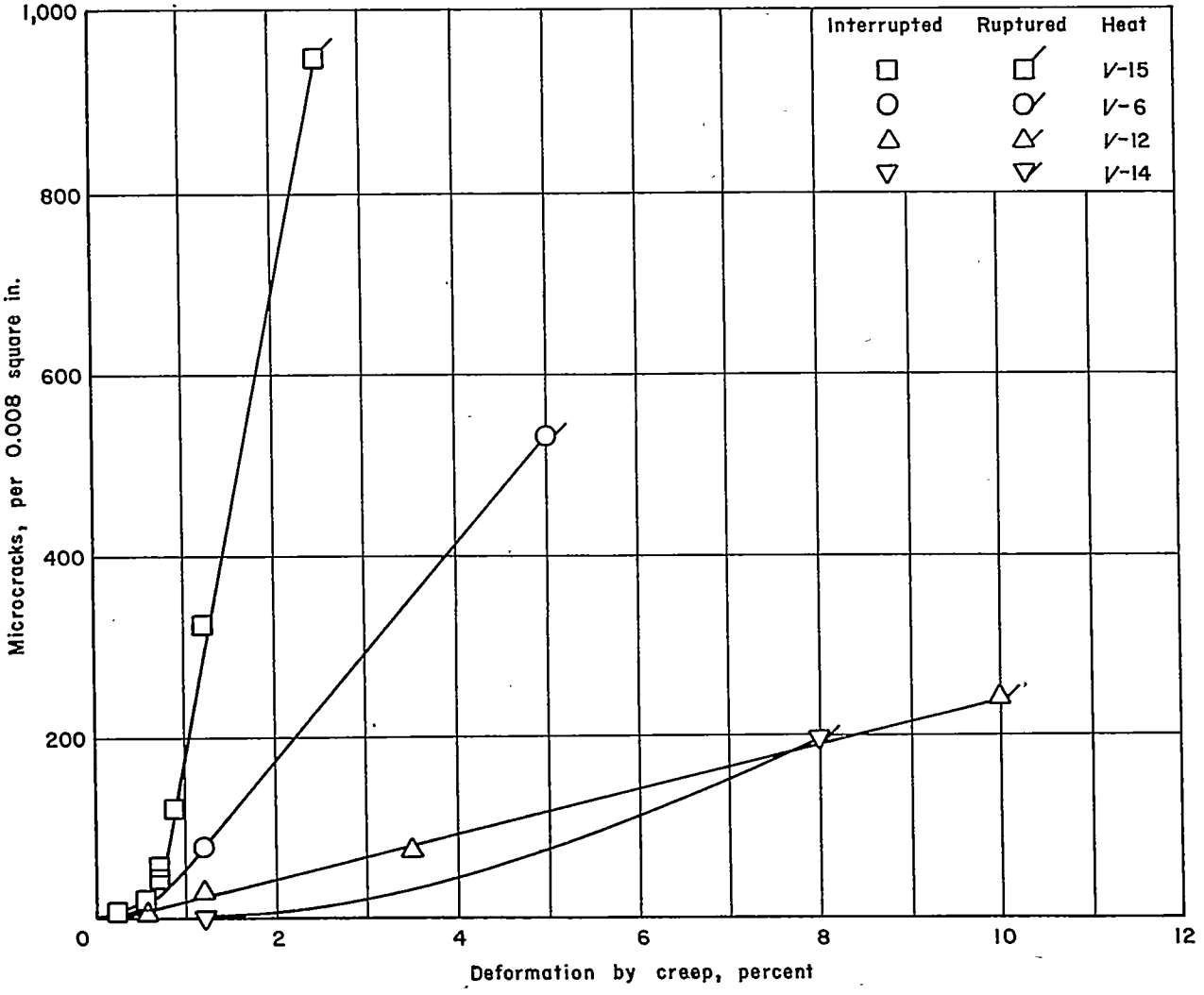

FIGURE 23.—Effect of creep deformation at 1,600° F on microcracking of specimens stressed to give comparable strain rates. Micrographs of of typical microcracks are shown. Tension axis was horizontal to electron micrograph.

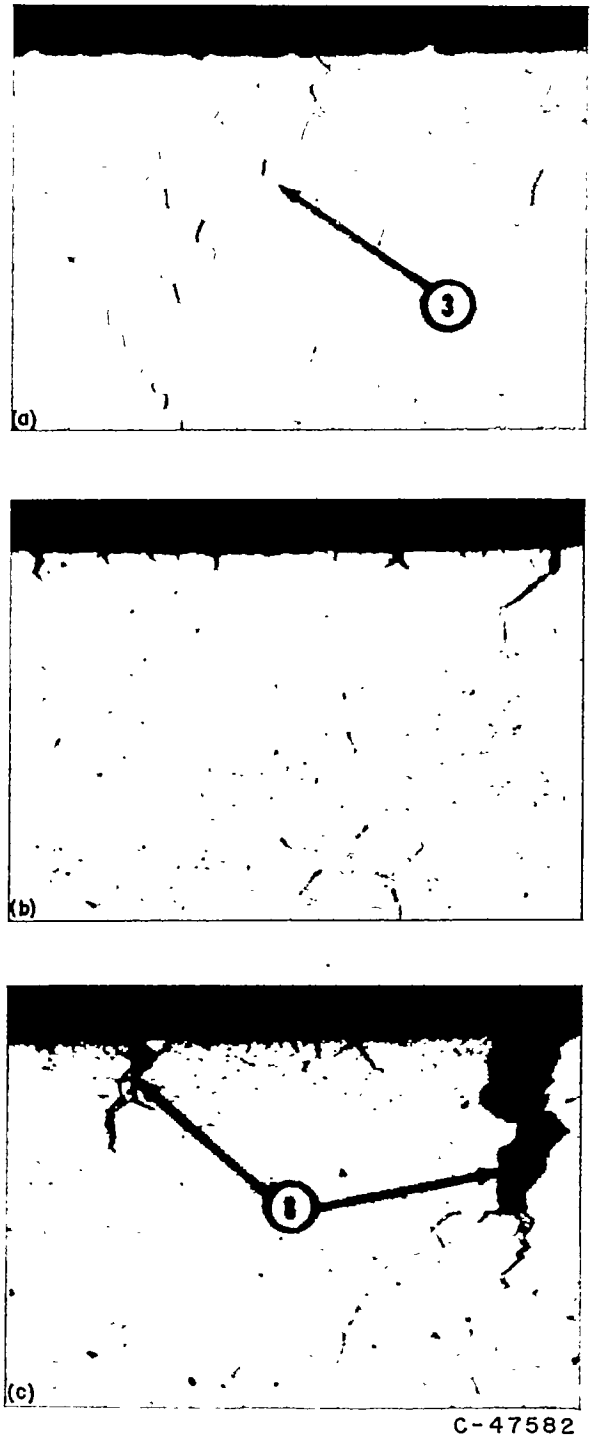

(a) Heat V–15; ruptured in 52 hours at 1,600° F and 25,000 psi; 13 surface cracks and 376 microcracks.
(b) Heat V–12; ruptured in 296 hours at 1,600° F and 28,000 psi; 160 surface cracks and 243 microcracks.
(c) Heat V–14; ruptured in 266 hours at 1,600° F and 30,000 psi; 300 surface cracks and 198 microcracks.

FIGURE 24.—Change in mode of cracking. Surface cracks are number penetrating more than 0.003 inch per inch of specimen. Microcracks are number in 0.008 square inch. X32; 3, microcrack; 8, surface cracks.

V–12, and heat V–14. When the four heats were exposed 165 hours at 1,600° F and 20,000 psi, the difference in microcracking was even more pronounced. The counts showed 314 microcracks in the boron-and-zirconium-free heat V–15 while only 9 were present in the zirconium-bearing heat V–6 and none in the heats with boron or boron plus zirconium.

It was evident from the specimens tested at 1,600° F and 25,000 psi that, although the microcracking was retarded, it was not prevented by boron and zirconium (table VI).

Intergranular surface cracks.—In addition to microcracks within the specimens, the heats were subject to intergranular cracking from the specimen surface during creep-rupture tests. Initiation of these cracks was definitely from the specimen surface with a gradual increase in number and depth during creep exposure. Some of these cracks are illustrated in figure 24 which has quantitative data on amounts listed. This figure demonstrates that the specimen from the boron-and-zirconium-free heat V–15 tested at 1,600° F and 25,000 psi showed negligible surface cracking at the time of rupture, 52 hours. The mode of fracture by linking of the interior microcracks is also shown in this figure. However, in the boron-bearing heat V–12 tested at 1,600° F and 28,000 psi, the amount of microcracking was diminished but surface cracking had occurred. The importance of these surface cracks in fracture is indicated by the sample from the heat with boron plus zirconium (V–14) tested at 1,600° F and 30,000 psi, where some of the surface cracks penetrated more than ¼ of the specimen radius.

The quantitative data for surface cracks seem to indicate that the trace-element additions modified the mode of fracture. Surface cracking increasingly competed with microcracking as a source of fracture when the tendency for microcracking was reduced by zirconium and/or boron.

Intragranular precipitation of carbide.—In addition to a decreased tendency for the precipitation of intergranular $M_{23}C_6$-type carbides, boron caused carbides to precipitate intragranularly during exposure at 1,600° F (fig. 17).

The form of this phase was stress dependent. Short platelike carbides formed in samples aged without stress. In the samples aged under stress these were more elongated in form (cf. figs. 16 and 20) and had a tendency to precipitate on preferred matrix planes. As shown in figure 18 when these precipitates were extracted from the boron heat (V–12) after 1.2-percent creep strain in 188 hours at 1,600° F, the majority of spots in the electron-diffraction pattern indexed for M_6C with some spots corresponding to $M_{23}C_6$. Therefore, it seemed that some of the intragranular carbide phase, if not all, was M_6C rather than $M_{23}C_6$.

The intragranular carbide was distributed fairly uniformly throughout the grains in the heats with boron (V–12 and V–14) with some concentration near the Ti(C,N) particles.

There was some evidence that intragranular carbides diminished and carbides in the grain boundaries increased during long time exposure, which indicates that carbon was diffusing to the grain boundaries.

Intragranular γ'.—The intragranular precipitates of γ' grew and agglomerated during aging at 1,600° F. As measured by the surface density of γ' particles in electron micrographs there was no significant effect of boron, zirconium, or stress on this reaction (fig. 25). Therefore, the differences in surface density of γ' existing after the original heat treatment of air-cooling from 2,150° F were not lasting and appeared to be unimportant.

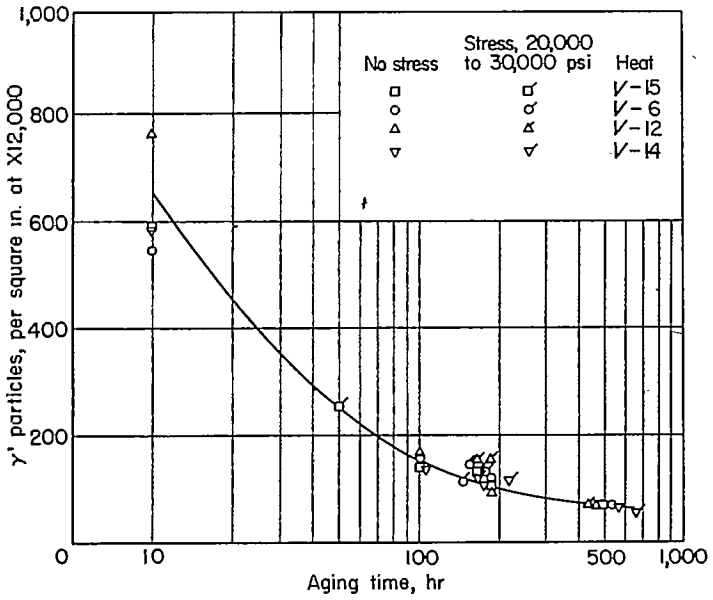

FIGURE 25.—Effect of aging time at 1,600° F with or without stress on γ' particle density.

As a further means of evaluating effects of trace elements on aging of γ' at 1,600° F, the change of hardness with aging time at 1,600° F was measured (fig. 26 and table VII). The hardness changes for the four experimental heats were very similar except that the heat with boron plus zirconium (V–14) aged to a higher hardness up to 500 hours. All heats reached maximum hardness at 1,600° F at about 1 hour and then overaged at longer times. Electron micrographs typical of the alloy showing γ' density are included in figure 26.

Although creep strain did not affect the density of γ' particles, it did modify the distribution of particles. Creep strains within the grains resulted in some preferential agglomeration of γ' on the slip planes, as evidenced by an alinement of γ'. This was especially noticeable after high creep strain (fig. 22).

Nodular precipitate.—All the heats exhibited nodules of a precipitate to some extent after aging at 1,600° F (fig. 27 and tables VI and VII). The nodules, which often were seen to envelop or abut on carbon-rich Ti(C,N) particles, appeared to be of mixed carbide and γ'. Their occurrence was definitely accelerated by strain, especially in the heat free from boron or zirconium (V–15). Likewise, they were trace-element controlled in that their formation was retarded by boron and zirconium.

Check of boron content after creep exposure.—A specimen from the heat with boron (V–12) was analyzed for boron content after rupture in 428 hours at 1,600° F and 25,000 psi. The cross section of the specimen showed 0.0090 percent boron. A surface layer of approximately 0.010-inch thickness contained 0.0079 percent boron. These analyses compared well with the analysis of 0.0089 percent boron obtained in the as-rolled bar stock.

Discussion.—The microstructural studies revealed the role of boron and zirconium in increasing creep-rupture life and ductility of the 55Ni-20Cr-15Co-4Mo-3Ti-3Al alloy.

In the absence of boron and zirconium, $M_{23}C_6$ and γ' particles rapidly formed a network in the grain boundaries of the alloy during creep at 1,600° F. This was followed by depletion of γ' precipitates in the metal adjacent to the transverse grain boundaries and early intergranular microcracking at the $M_{23}C_6$-depleted zone interfaces. The microcracks grew, linked, and initiated early fracture in a brittle manner. Boron and zirconium retarded this grain boundary process, thereby allowing longer creep exposure and higher creep deformation before the fracture mechanism operated.

Additional experimental support for the mechanism is obtained by relating creep-rupture life and ductility (fig. 28) at 1,600° F and 25,000 psi to the tendency of the experimental heats to undergo depletion of grain boundaries and microcracking during 1.2-percent creep deformation in 165 to 214 hours at 1,600° F.

It is evident from the data that the increase in creep-rupture life and ductility from the trace-element addition results from retardation, but not prevention, of the grain-boundary mechanism of carbide formation, grain-boundary depletion, and microcracking. The specimens from all the experimental heats were similar in these respects after rupture at 1,600° F and 25,000 psi. However, both the time and deformation at which the grain-boundary effects occurred and initiated fracture were increased by boron and zirconium.

The finding that boron and zirconium retards the microcracking process does not imply that their beneficial effects are only temporary in nickel-base alloys. All available data indicate that the heats containing boron and zirconium are superior to those free of boron and zirconium even at low stresses and long time exposure.

The chemical analyses on heat V–12 after rupture-testing indicated that loss of boron from the sample during testing did not occur except possibly at the surface. Deboronization does not appear to be the cause of the eventual appearance of the grain-boundary changes in boron-bearing materials.

Interpretation of other microstructural changes: Apparently the occurrence of intragranular carbide in the heats with boron was related to retardation of $M_{23}C_6$ agglomeration in the grain boundaries. In a sense, a redistribution of carbide was effected by boron. While zirconium addition suppressed the grain-boundary agglomeration, it did not cause formation of intragranular carbides.

The intragranular carbide in the boron heats may have had a direct effect on properties in addition to tying up carbon to retard $M_{23}C_6$ agglomeration in grain boundaries. The form of the precipitate after creep indicates that it is strain-induced and may lower creep rate in a manner proposed by Cottrell (ref. 23). According to Cottrell, resistance to creep is obtained by nucleation and growth of precipitates in dislocations, which prevent further movement of the dislocations through the lattice. The reaction would resemble strain-aging, although the resulting precipitate would be more advanced in growth than that usually associated with strain-aging.

The negative creep and slight serrated effect in the creep curves of the boron heats at 1,600° F and 20,000 psi appear to be additional evidence of strain-induced precipitation. These phenomena have been observed in unpublished work

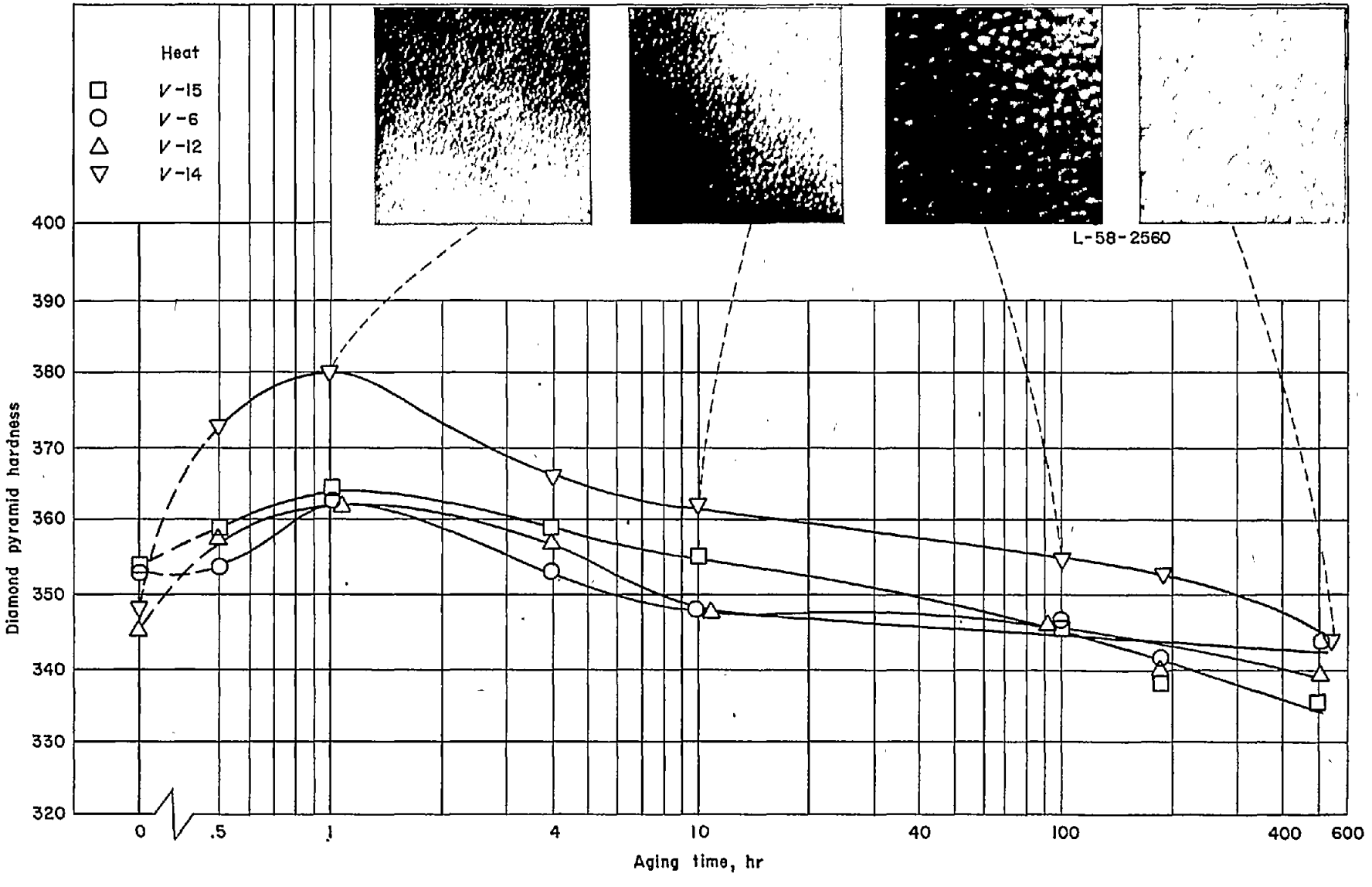

FIGURE 26.—Effect of aging at 1,600° F without stress on hardness and γ' dispersion. Typical electron micrographs at X12,000 show γ' dispersion.

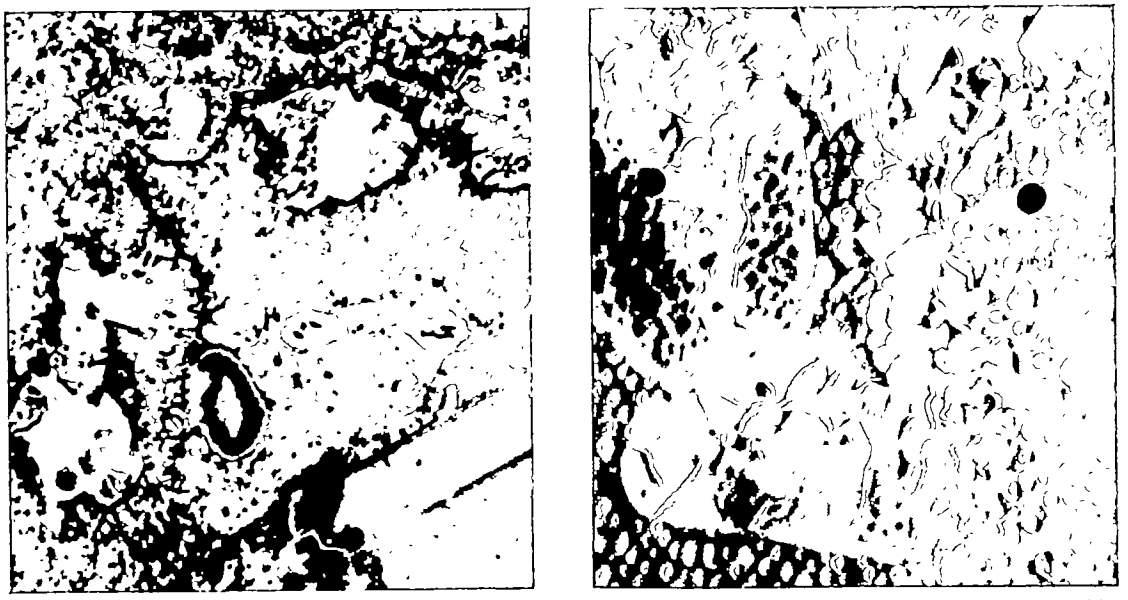

C-47591

X2,000
Light micrograph

X12,000
Electron micrograph

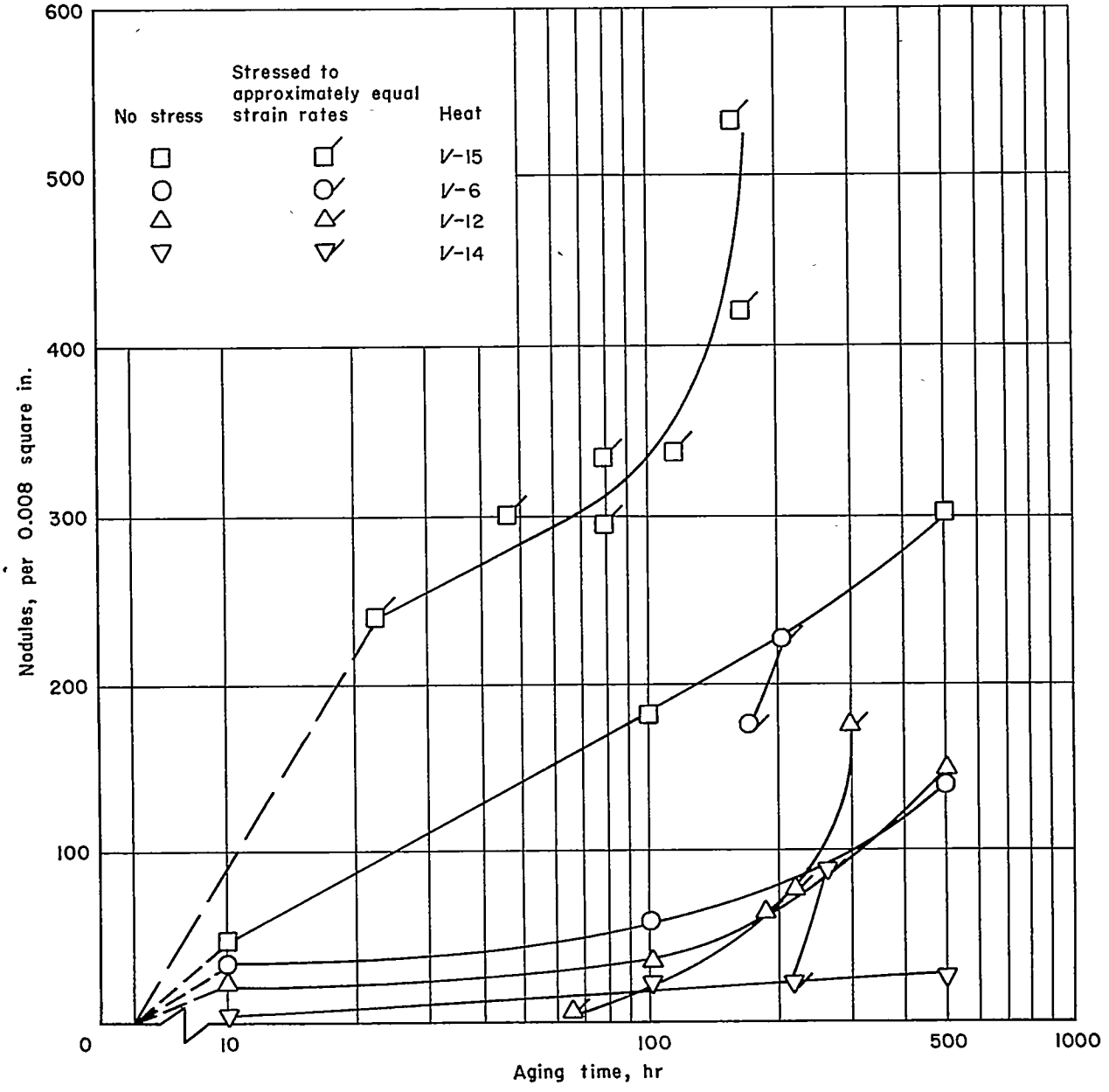

FIGURE 27.—Effect of aging time at 1,600° F on nodule density. Micrographs of typical nodules are shown.

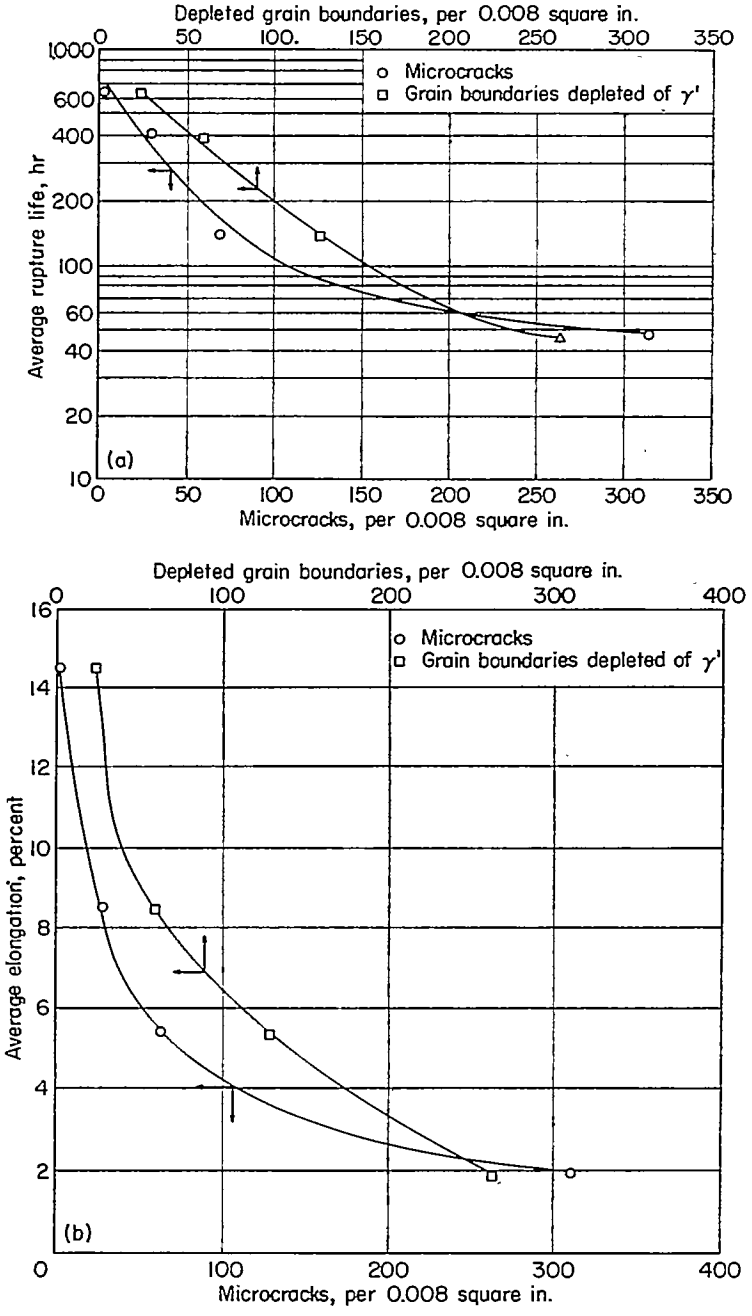

(a) Rupture life.
(b) Elongation.

FIGURE 28.—Relation of rupture life and elongation at 1,600° F and 25,000 psi to microcracking and γ' depletion tendencies at grain boundaries measured after 1.2-percent deformation in 165 to 214 hours.

in this laboratory in other nickel-base alloys containing boron. The presence of strain-aging-type reactions in nickel-base alloys is not totally unexpected in that Waché (ref. 24) has detected serrated stress-strain curves for 80Ni–20Cr alloys at temperatures up to 1,292° F. Although the above evidence indicates that a strain-induced carbide precipitate might have lowered creep rate, the proof was not considered positive.

The depletion of γ' definitely required stress. No evidence of its occurrence was observed in any case of exposure to 1,600° F without stress. In addition, depletion was more prevalent in the transverse grain boundaries. The absence of γ' depletion when the alloy was aged at 1,600° F without stress indicates that the reaction was not due to simple depletion of elements forming γ' from the adjoining matrix by the grain-boundary precipitates. It seems probable that localized strain concentration at the grain boundaries during creep induced γ' agglomeration.

The information obtained on surface cracking was not sufficiently extensive for one to be sure of its role. The indications were that when boron or zirconium retarded microcracking to allow longer creep exposures or more highly stressed creep exposures, fracture was at least in part initiated by surface cracks.

It was initially thought that boron and zirconium might operate through some influence on the size, distribution, or stability of the intragranular γ' reaction. Since Baillie (ref. 14) succeeded in correlating creep-rupture properties with the surface density of γ' particles as measured in electron micrographs, surface density was used to detect possible effects of boron and zirconium on the γ' which would increase rupture life. No significant effect was found. In fact, these elements had so little effect on any aspect of γ' (other than in suppressing agglomeration and depletion of γ' at grain boundaries) that it seems certain that the boron-zirconium effect did not operate in this manner.

In the absence of any observable effect of boron or zirconium on the γ' precipitates the reason for the higher hardness of the heat with boron plus zirconium (V–14) is uncertain. It was noted that the hardness values were in the same order as the total titanium plus aluminum in the heats. The slightly higher titanium-plus-aluminum content may account for the higher hardness of heat V–14.

The distribution of the γ' after creep exposure was found to be a good indicator of the mode and location of creep deformation. Alinement of γ' seemed to indicate that creep deformation had been accommodated within the grains as coarse slip. This alinement had previously been shown by Bueckle and Poulignier (ref. 25) to indicate the mode of deformation in nickel-base alloys.

The role of the nodules of mixed carbide and γ' was not clear. No evidence was found to indicate that cracking was initiated by their presence. It is possible that the nodules contributed to the depletion of γ' from the matrix adjacent to the grain boundaries by acting as a final location for the γ'. This hypothesis is somewhat supported by the accelerating effect of stress on nodule formation at 1,600° F, particularly when γ' depletion occurred.

Relation of mechanism to published information: The accumulation of $M_{23}C_6$ carbide in grain boundaries has striking parallels to sensitization of stainless steels. Simpkinson (ref. 26) and Bungardt and Lennartz (ref. 27) have identified $Cr_{23}C_6$ as the grain-boundary phase leading to stress corrosion of 18–8 stainless steels. In addition, Plateau, Henry, and Crussard (ref. 20) found the size, shape, and distribution of $Cr_{23}C_6$ in 18–8 stainless steels to be similar to that of $M_{23}C_6$ found in this study.

The agglomeration at grain boundaries during creep of nickel-base alloys hardened with titanium and aluminum has been noted by Baillie and Poulignier (ref. 28) and Mathieu

(ref. 29). Mathieu hypothesized that the precipitate was γ' and chromium compounds. Although it was stated that this agglomeration was probably important in determining rupture life, further details on the mechanism were not given.

In accordance with the theories of Chang and Grant (ref. 30), depletion of precipitates in layers of matrix adjacent to grain boundaries would promote microcracking and fracture by concentrating deformation at these weak grain boundaries. It is possible that this mechanism operates in many high-temperature alloys to give brittle fractures when the creep resistance of the material remains high. Such an explanation was offered by Wever and Schrader (ref. 31) for brittle fracture of Cr-Ni-Mo steels in long-time service at 500° C. They found that localized precipitation of Mo_2C from the matrix adjacent to the grain boundaries left a condition of strong grains and depleted grain boundaries. Further confirmation is obtained from work on the effect of cellular precipitation (refs. 32 and 33) where this resulted in depleted regions in the grain boundaries and led to premature and brittle rupture by creep.

The location of microcracks at the $M_{23}C_6$ precipitate matrix interface was interesting in light of the work of Resnick and Seigle (ref. 34), who established that zinc oxide particles were heterogeneous nuclei for microcracks in α-brass. As shown by Machlin (ref. 35), particle-matrix bonding is important in nucleation of microcracks. In general, the presence of second-phase particles makes nucleation more probable, especially when bonding is poor. Considering these effects, it seems probable that the $M_{23}C_6$ particles acted as nuclei for microcracks, possibly because of poor bonding.

The mechanism of nucleation and growth of microcracks is not clear. Several authors (refs. 34, 35, 36, 37, and 38) have proposed condensation of vacancies formed during creep by dislocation movements; others (refs. 30, 39, and 40) emphasized local stress concentrations as the cause. Grain-boundary sliding is usually considered to set up the local stress concentrations at the transverse boundaries to cause loss of cohesion. Chang and Grant (ref. 30) hypothesize that the rate of growth of microcracks in grain boundaries depends upon the stress pattern at the boundaries. Propagation of microcracking is caused primarily by the normal stress at the grain boundary and the inability of the material to relieve this stress. The overall rate of growth depends upon the ability of the grains to accommodate the normal stresses by deformation within the grain. From this it can be inferred that microcracking increases as the severity of localization of deformation at grain boundaries increases. Therefore, change of the mode of deformation from intragranular slip to grain-boundary creep can be expected to increase grain-boundary microcracking by redistribution of stresses. In fact, in α-brass the occurrence of microcracking is coincident with the change from coarse slip to grain-boundary sliding (ref. 36). The evidence of increased intragranular slip and decreased microcracking in the heats with boron and zirconium is in full agreement with the above theories. It appears feasible that the elements have changed the mode of deformation by maintaining the grain-boundary strength.

The discrepancies in the literature on the time of microcrack nucleation are not surprising, considering the effect of trace elements in this study. While several instances have been found of microcracking early in second-stage creep (refs. 37, 41, and 42), other cases exist where none was found until tertiary creep (refs. 36, 43, and 44). In the present study, the case exists where, on one alloy, nucleation of microcracks was delayed from late in first-stage creep to third-stage creep by trace elements.

Regarding the effect of microcracks on properties, the Russian theorists (refs. 38, 42, and 45) attribute tertiary creep and rupture to a gradual destruction of the metal by microcracking. This implies that microcracking raises creep rate and lowers life and ductility. In addition, the normal break in the stress-rupture curve of commercial alloys associated with a change from transgranular to intergranular fracture is an important consideration. This change in fracture mechanism, which is essentially an increase in intergranular microcracking, results in lower life and ductility than predicted from higher stress data where microcracking was less predominant.

Causes of effect of boron and zirconium on grain-boundary stability: The experimental evidence established that trace amounts of boron and zirconium retard agglomeration at grain boundaries and thereby retard the microcracking mechanism. Several causes of this retardation of agglomeration might be proposed.

A possibility would be that the trace elements promote stabilization of carbon indirectly by promoting the nucleation and growth of one carbide at the expense of another. This might result from solid solution of boron or zirconium in the complex carbides of the M_6C or $M_{23}C_6$ type. Indeed the detection of intragranular carbides, apparently of the M_6C type, when boron was present is compatible with this hypothesis. However, lack of promotion of additional carbides by zirconium additions does not support this hypothesis.

An alternative reason might be found in equilibrium segregation. Cahn (ref. 46) has reviewed the relationships of grain boundaries to impurity distribution. When elements of odd atomic size exist in alloys, they are subject to inhomogeneous distribution. Because they do not fit well in the crystal lattice where high regularity exists, the odd-sized atoms segregate to regions of lower regularity where larger vacancies exist. Grain boundaries are a prime region of concentration because of their inherent irregularity. Experimental confirmation for this was obtained by Thomas and Chalmers (ref. 47) who found that polonium segregates to grain boundaries in lead-bismuth alloys.

The segregating tendencies of two competing odd-sized elements can be related to their degree of misfit in that the most odd-sized atoms will seek the grain boundary most rapidly. Thus, small amounts of one very odd-sized element can be utilized to heal the grain boundary, thereby retarding the segregation of a less odd-sized element by decreasing the available flaws in the grain boundary. The possibility exists that boron and zirconium are retarding carbon segregation by this mechanism.

Study of the atomic diameters of carbon, boron, and zirconium might reveal the feasibility of this. Speiser, Spretnak, and Taylor (ref. 48) have shown that the effective diameter of carbon γ-Fe is 1.36 angstrom units, while they postulate that boron has an effective diameter equivalent to or greater than 1.85 to 1.90 angstrom units. Goldschmidt's

metallic diameter (for coordination number of 12) for zirconium is 3.20 angstrom units. The available lattice spaces in the 55Ni–20Cr–15Co–4Mo–3Ti–3Al alloy can be calculated from the lattice parameter of 3.58 angstrom units established in unpublished work at this laboratory. The vacant interstitial space in solid solution is 1.05 angstrom units in diameter. Using the data on atomic diameters, the carbon atom is 30 percent larger, boron is 78 percent larger, and zirconium is 200 percent larger than the available space. In the case of substitutional solution, the boron atom is approximately 26 percent smaller, and zirconium 26 percent larger than the substitutional space with a 2.53-angstrom-unit diameter. Therefore, it appears that carbon fits moderately well interstitially but that boron and zirconium fit poorly both as interstitials and in substitution. Then it seems feasible that boron and zirconium are segregating preferentially to grain boundaries, healing them and retarding carbon segregation.

Other aspects of the data lend support to the theory of equilibrium segregation. Decreased tendency for γ' agglomeration at the grain boundaries in the boron and zirconium heats could result from the boron and zirconium healing the grain boundaries. The promotion of intragranular carbide by boron might be the indirect result of this. The decreased segregation would leave a higher carbon content within the grains, making precipitation of intragranular carbides more probable.

Additional support for the theory of equilibrium segregation is in the literature. Brown (ref. 49) proposed that boron additions beneficiated iron-base alloys by this mechanism. Strauss (ref. 2) emphasized that marked beneficiation of properties by trace-element additions usually occurs with elements with characteristics which would lead to segregation to grain boundaries.

Role of carbon: The apparent harmful effect of $M_{23}C_6$ in the grain boundaries of the alloy and the possible helpful effect of the intragranular carbide promoted by boron make the role of carbon in nickel-base alloys of great interest.

One might conclude from the results that a relatively carbon-free alloy would be free of the grain-boundary carbide agglomeration and, therefore, have properties equivalent to the heat with boron plus zirconium (V–14). This, however, is not the case. It has been shown in unpublished work at this laboratory that both rupture life and ductility increase as carbon is increased from less than 0.01 to 0.04 percent in the boron- and zirconium-free alloy. Therefore, it seems that carbon can also have a beneficial role in the alloy. The reason for this effect is not at all clear at this time but it could be one of several mechanisms including improved degassing, solid-solution strengthening, or prevention of other embrittling grain-boundary reactions.

Generality of results: The beneficial effects of boron and zirconium in nickel-base titanium-plus-aluminum refractory alloys is common knowledge. Therefore, it follows that properties of such alloys in the absence of these elements will generally be inferior to their properties when the proper amounts are present. The particular alloy used to study the boron-zirconium mechanism is certainly not unusual in this respect. The results presented do in fact increase the confidence which can be placed in the alloy studied through clarification of the mechanism involved.

It is confidently expected that the basic mechanism established for the influence of trace amounts of boron and zirconium will be generally applicable. However, there will be variants in individual alloys and within a specific alloy depending on prior history, heat treatment, and testing conditions. With this in mind, the limitations of the present results should be clearly recognized. Only one alloy with one heat treatment was studied. The test conditions were limited to 1,600° F on material made in a small vacuum furnace and hot-worked under idealized laboratory conditions.

In the type of alloy considered it is expected that boron and zirconium will generally be found to suppress the formation of noncoherent phases in grain boundaries and the weakening of the adjacent matrix material through depletion of γ'. Both the details of the mechanism and the effectiveness can be expected to vary depending on the major alloying elements in specific alloys and the variations of other elements in trace amounts. Because such factors as grain size, carbide composition and distribution, and cold-work are prior-history sensitive, the effectiveness of the boron and zirconium can be expected to vary with the basic microstructure of the alloy. It should be recognized that the boron and zirconium must be present in an effective form. For instance, they must be added under conditions in which their effectiveness is not nullified by reaction with oxygen or nitrogen.

The mechanism of creep can be expected to vary with test temperatures and stress. Conditions which favor creep within the grains (temperatures on the low side of the creep range and high stresses) apparently would reduce the effectiveness of boron and zirconium under the mechanism observed. Variations in the conditions of formation of γ' or in the amounts through variation in titanium and aluminum would also be involved. It is becoming evident through the research efforts of others that the type of carbide formed can be temperature and time dependent. Again this would alter the effectiveness of the boron-zirconium reaction.

It was shown by figure 10 that there can be sharp optimums in the properties depending on the amounts of boron plus zirconium. This aspect of the mechanism has not yet been established although it is expected that it will arise from some modification of the observed mechanism. It was also shown that boron and zirconium up to limiting amounts were very effective in reducing cracking during hot-working. This demonstrates that they are effective at temperatures much higher than 1,600° F. It is not certain if the same mechanism as that observed at 1,600° F is involved.

Boron, at least, is effective in raising creep-rupture properties of alloys other than the nickel-base alloys containing titanium plus aluminum. The results of this investigation suggest that it may operate in these cases through modification of carbide reactions. The further possibility also exists that boron, by itself or through modification of carbon-nitrogen reactions, introduces strain-aging-type reactions.

CONCLUSIONS

The following conclusions can be drawn from the present investigation of the effects of trace elements in a complex heat-resistant alloy:

1. The type of ceramic crucible used was an important variable in induction vacuum melting of a 55Ni-20Cr-15Co-4Mo-3Ti-3Al heat-resistant alloy. Properties at high temperature and hot-workability were found to be markedly improved when 10 to 20 parts per million of boron were introduced into the heats as a result of reaction between the melt and magnesia crucibles due to the usual contamination of magnesia with boron compounds. Zirconium derived from reaction with zirconia also improved properties but to a lesser extent than boron. Heats melted in alumina had poor properties and hot-workability because neither boron nor zirconium were introduced into the heats.

2. The finding that trace amounts of boron or zirconium derived from reaction between the melt and crucible refractories were so influential on properties appears to explain many of the variabilities encountered in producing alloys by induction vacuum melting. The experience in the laboratory indicates that the amounts introduced by reaction with refractories can vary from practically none to amounts improving properties to a substantial degree. The conditions of melting which control the pickup of boron and zirconium are not understood.

3. Apparently trace amounts of boron or zirconium are necessary for usable properties and hot-workability. Boron and/or zirconium have had to be present in the alloy studied to attain the properties considered characteristic of the alloy. When good properties were obtained without knowingly adding these elements, they were introduced unknowingly by crucible reaction or in the charge. Therefore, good metallurgical practice appears to require that the optimum amounts be specifically added.

4. Deliberate simultaneous additions of boron and zirconium indicate that there are interaction effects leading to optimum amounts for best properties and hot-workability. Better properties were obtained by simultaneous additions of certain amounts of the two elements than by adding either singly. Excessive amounts led to poor hot-workability and reduced properties.

5. The improvement in creep-rupture properties was found to be due to the ability of zirconium, boron, and optimum amounts of boron plus zirconium, in that order of effectiveness, to retard structural deterioration at the grain boundaries. In the absence of boron or zirconium, creep at 1,600° F caused agglomeration of $M_{23}C_6$ type carbides at the grain boundaries normal to the applied stress. The adjacent matrix became depleted of the γ' precipitate which provides the basic strength of the alloy. Microcracks formed at the interface of the $M_{23}C_6$ particles and the matrix weakened by the depletion of γ' grew and linked together to cause early brittle fracture.

6. Zirconium retarded this process. Boron was more effective and the optimum amount of boron plus zirconium was most effective. The rupture life was improved through decreased rate and increased duration of secondary creep, as well as by a marked increase in the amout of tertiary creep before fracture. The appearance of microcracks was shifted from late in primary creep for material without boron or zirconium until well into tertiary-stage creep for material with optimum boron plus zirconium. Boron appeared to be most effective because it shifted the initial carbide precipitation from the grain boundaries to within the grains in the form of M_6C rather than $M_{23}C_6$ compounds.

University of Michigan,
Ann Arbor, Mich., *August 5, 1958.*

REFERENCES

1. Koffler, R. W., Pennington, W. J., and Richmond, F. M.: The Effect of Small Amounts of Boron and Zirconium on the High Temperature Properties of Vacuum-Melted Super Alloys. Rep. 48, Res. and Dev. Dept., Universal-Cyclops Steel Corp., June 11, 1956.
2. Strauss, J.: Micrometallurgy—The Metallurgy of Minute Additions. Proc. ASTM, vol. 53, 1953, pp. 577–595.
3. Mudge, W. A.: The Melting of Nickel. Nonferrous Melting Practice. Inst. Met. Div. Symposium Ser., AIME (New York), 1946, pp. 74–78.
4. Martin, L. H., and Bieber, L. O.: Methods of Evaluating Hot Malleability of Nickel and High-Nickel Alloys. Vol. II, Nonferrous Rolling Practice. Inst. Met. Div. Symposium Ser., AIME (New York), 1948, pp. 15–31.
5. Bieber, C.: The Melting and Hot Rolling of Nickel and Nickel Alloys. Metals Handbook, ASM (Cleveland), 1948, pp. 1028–1029.
6. Darmara, F. N.: Quality Control Achieved by Vacuum Melting and Effects on High Temperature Properties. Paper presented at Regional High-Temperature Materials Conf., Cleveland Sec. of AIME, Apr. 17, 1957.
7. Jones, W. E.: Vacuum Induction Melting-Process Considerations. Metal Prog., vol. 72, no. 4, Oct. 1957, pp. 133–138, 220–222.
8. Nordheim, R., and Grant, N. J.: Aging Characteristics of Nickel-Chromium Alloys Hardened with Titanium and Aluminum. Jour. Metals, vol. 6, no. 2, sec. 2 (Trans.), Feb. 1954, pp. 211–218.
9. Taylor, A.: Constitution of Nickel-Rich Quaternary Alloys of the Ni-Cr-Ti-Al System. Jour. Metals, vol. 9, no. 1, sec. 2 (Trans.), Jan. 1957, pp. 71–75.
10. Betteridge, W., and Franklin, A. W.: Les Progrès des alliages à base de nickel-chrome en service à haute température. Rev. métallurgie, t. 53, pt. 4, Apr. 1956, pp. 271–284.
11. Frey, D. N., Freeman, J. W., and White, A. E.: Fundamental Aging Effects Influencing High-Temperature Properties of Solution-Treated Inconel X. NACA TN 2385, 1951.
12. Brockway, L. O., and Bigelow, W. C.: The Investigation of the Minor Phases of Heat-Resistant Alloys by Electron Diffraction and Electron Microscopy, WADC TR 54–589, Contract AF–33(616)–23, WADC and Univ. of Mich., May 1955.
13. Betteridge, W., and Smith, R. A.: Effect of Heat Treatment and Structure Upon Creep Properties of Nimonic Alloys Between 750° and 950° C. Symposium on Metallic Materials for Service at Temperatures Above 1,600° F. Special Tech. Pub. No. 174, ASTM, 1956, p. 29.
14. Baillie, Y.: Quelques résultats de l'étude au microscope électronique des alliages Ni-Cr-Al-Ti employés dans les turbines aeronautiques. Revue Univ. des Mines, t. 12, no. 10, ser. 9, Oct. 1956, pp. 507–512.
15. Beattie, H. J., and VerSnyder, F. L.: The Influence of Molybdenum on the Phase Relationships of a High Temperature Alloy. Trans. ASM, vol. 49, 1957, pp. 883–895.
16. Wilde, Robert F., and Grant, Nicholas J.: Aging in Complex Commercial Ni-Cr Alloys Hardened with Titanium and Aluminum. Jour. Metals, vol. 9, no. 7, sec. 2 (Trans.), July 1957, pp. 865–872.

17. Betteridge, W., and Franklin, A. W.: The Effect of Heat-Treatment and Structure on the Creep and Stress-Rupture Properties of Nimonic 80A. Jour. Inst. Metals, vol. 85, pt. II, 1957, pp. 473–479.
18. Bigelow, W. C., Amy, J. A., and Brockway, L. O.: Electron Microscopic Identification of the γ' Phase of Nickel-Base Alloys. Proc. ASTM, vol. 56, 1956, pp. 945–953.
19. Fisher, R. M.: Electron Microstructure of Steels by Extraction Replica Technique. Symposium on Techniques for Electron Metallography. Special Tech. Pub. No. 155, ASTM, 1953, pp. 49–63.
20. Plateau, J., Henry, G., and Crussard, C.: Quelques nouvelles applications de la microfractographie. Rev. mètallurgie, t. 54, pt. 3, Mar. 1957, pp. 200–216.
21. Bradley, D. E.: Evaporated Carbon Films for Use in Electron Microscopy. Brit. Jour. Appl. Phys., vol. 5, Feb. 1954, pp. 65–66.
22. Fullam, Ernest F.: Replica Washing Methods. Symposium on Techniques for Electron Metallography. Special Tech. Pub. No. 155, ASTM, 1953, pp. 101–108.
23. Cottrell, A. H.: Creep and Ageing Effects in Solid Solutions. Symposium on Creep and Fracture of Metals at High Temperatures (May 31–June 2, 1954), Nat. Phys. Lab. (London), 1956, pp. 141–152.
24. Waché, Xavier: Allongement discontinu des austénites soumises à l'essai de traction ordinaire à hautes températures. Comp. rend., Acad. Sci. (Paris), t. 240, May 1955, pp. 1892–1896.
25. Bueckle, C., and Poulignier, J.: Étude métallographique de l'écrouissage dans les alliages du type nickel-chrome, 80/20 tenaces à chord. Rev. métallurgie, t. 53, pt. 3, Mar. 1956, pp. 179–188.
26. Simpkinson, T. V.: Metallography of Titanium-Stabilized 18–8 Stainless Steels. Trans. ASM, vol. 49, 1957, pp. 721–746.
27. Bungardt, Karl, and Lennartz, Gustav: Ausscheidungsvorgänge in einem mit Titan stabilisierten austenitischen Chrom-Nickel-Stahl und ihre Beziehung zur interkristallinen Korrosion. Archiv Eisenhuttenwesen, Jahrg. 27, Heft 2, Feb. 1956, pp. 127–133.
28. Baillie, Y., and Poulignier, J.: Etude de la précipitation submicroscopique dans les alliages refractaires nickel-chrome. Rev. métallurgie, t. 51, pt. 3, Mar. 1954, pp. 179–191.
29. Mathieu, M.: Contribution à la connaissance des alliages Ni-Cr 80/20 modifies resistant à chaud. La Recherche Aero., no. 51, May-June 1956, pp. 43–51.
30. Chang, H. C., and Grant, Nicholas J.: Mechanism of Intercrystalline Fracture. Jour. Metals, vol. 8, no. 5, sec. 2 (Trans.), May 1956, pp. 544–551.
31. Wever, Franz, and Schrader, Angelica: Elektronenmikroskopische Untersuchung der Gefügeveränderungen eines Chrom-Nickel-Molybdän-Stahles unter langzeitiger Zugbeanspruchung bei 500°. Archiv Eisenhuttenwesen, Jahrg. 26, Heft 8, Aug. 1955, pp. 475–481.
32. Roberts, C. S.: Interaction of Precipitation and Creep in MG–Al Alloys. Jour. Metals, vol. 8, no. 2, sec. 2 (Trans.), Feb. 1956, pp. 146–148.
33. Sully, A. H.: Discussion of Papers by C. H. M. Jenkins and W. Betteridge. Symposium on Creep and Fracture of Metals at High Temperatures (May 31–June 2, 1954), Nat. Phys. Lab. (London), 1956, p. 308.
34. Resnick, R., and Seigle, L.: Nucleation of Voids in Metals During Diffusion and Creep. Jour. Metals, vol. 9, no. 1, sec. 2 (Trans.), Jan. 1957, pp. 87–93.
35. Machlin, E. S.: Creep-Rupture by Vacancy Condensation. Jour. Metals, vol. 8, no. 2, sec. 2 (Trans.), Feb. 1956, pp. 106–111.
36. Greenwood, J. N., Miller, D. R., and Suiter, J. W.: Intergranular Cavitation in Stressed Metals. Acta Metallurgica, vol. 2, no. 2, Mar. 1954, pp. 250–258.
37. Crussard, C., and Friedel, J.: Theory of Accelerated Creep and Rupture. Symposium on Creep and Fracture of Metals at High Temperatures (May 31–June 2, 1954), Nat. Phys. Lab. (London), 1956, pp. 243–262.
38. Guy, A. G.: Russian Theory for Creep Fracture. Metal Prog., vol. 69, no. 3, Mar. 1956, pp. 158–160.
39. McLean, D.: A Note on the Metallography of Cracking During Creep. Jour. Inst. Metals, vol. 85, pt. II, July 1957, pp. 468–471.
40. Nield, B. J., and Quarrell, A. G.: Intercrystalline Cracking in Creep in Some Aluminum Alloys. Jour. Inst. Metals, vol. 85, pt. II, July 1957, pp. 480–485.
41. Nield, B. J.: Discussion of Papers by C. H. M. Jenkins and W. Betteridge. Symposium on Creep and Fracture of Metals at High Temperatures (May 31–June 2, 1954), Nat. Phys. Lab. (London), 1956, pp. 308–311.
42. Kishkin, S. T.: Mechanism of Weakening and Fracture of Crystalline Bodies as a Function of Time at High Temperature. Doklady Akad. Nauk SSSR, vol. 95, 1954, pp. 789–791.
43. McAdam, D. J., Jr., Giel, G. W., and Woodard, D. H.: Influence of Strain Rate and Temperature on the Mechanical Properties of Monel Metal and Copper. Proc. ASTM, vol. 46, 1946, pp. 902–950.
44. Kirkby, H. W.: Discussion of "Grain Boundary Participation in Creep Deformation and Fracture," by N. J. Grant. Symposium on Creep and Fracture of Metals at High Temperatures (May 31–June 2, 1954), Nat. Phys. Lab. (London), 1956, p. 331.
45. Dekhtiar, I. I., and Osipov, K. A.: Fracture of Metals at High Temperatures. Doklady Akad. Nauk SSSR, vol. 104, no. 2, 1955, pp. 229–232.
46. Cahn, R. W.: Grain Boundaries, Substructures and Impurities. ASM Seminar on Impurities and Imperfections, Thirty-sixth Nat. Metal Congress and Exposition (Chicago), Oct. 30–Nov. 5, 1955, pp. 41–83.
47. Thomas, W. R., and Chalmers, B.: The Segregation of Impurities to Grain Boundaries. Acta Metallurgica, vol. 3, no. 1, Jan. 1955, pp. 17–21.
48. Speiser, Rudolph, Spretnak, J. W., and Taylor, W. J.: Effective Diameter of Solute Atoms in Interstitial Solid Solution. Trans. ASM, vol. 46, 1954, pp. 1168–1175.
49. Brown, J. T., and Bulina, J.: W-545—A New High Temperature Turbine Disc Alloy. Paper presented at Regional High-Temperature Materials Conf., Cleveland Sec. of AIME, Apr. 16, 1957.

TABLE I

MELTING PRACTICE FOR EXPERIMENTAL HEATS

Heat	Crucible	Heat in crucible	Refining time, min	Refining temperature, ° F	Deoxidant	Superheat temperature, ° F	Pouring temperature, ° F	Addition, percent
V-1	Zirconia	1	0	-----	C in charge	3, 050	3, 000	----------
V-2	Zirconia	2	0	-----	C in charge	3, 050	3, 000	----------
V-3	Zirconia	1	20	2, 700	C in charge plus chunk C	3, 000	3, 000	----------
V-4	Zirconia	1	20	2, 700	Chunk C	2, 900	2, 900	----------
[a] V-5	Zirconia	2	20	2, 700	Chunk C	2, 950	2, 950	----------
V-6	Zirconia	3	20	2, 700	Al	3, 100	3, 000	----------
V-7	Zirconia	4	20	2, 700	Si	2, 975	2, 975	----------
V-8	Zirconia	1	20	2, 700	Al	2, 975	2, 750	----------
V-9	Zirconia	2	20	2, 700	Al	2, 750	2, 750	----------
V-10	Zirconia	3	20	2, 900	Al	3, 100	3, 000	----------
V-11	Magnesia	1	0	-----	C in charge	3, 000	3, 000	----------
V-12	Magnesia	2	0	-----	C in charge	3, 000	3, 000	0. 01B
V-13	Alumina	1	0	-----	C in charge	3, 000	3, 000	----------
V-14	Zirconia	1	0	-----	C in charge	3, 000	3, 000	. 01B
V-15	Alumina	1	0	-----	C in charge	3, 000	3, 000	----------
V-16	Alumina	2	0	-----	C in charge	3, 000	3, 000	. 15Zr
V-17	Alumina	3	0	-----	C in charge	3, 000	3, 000	. 01B
V-18	Alumina	4	0	-----	C in charge	3, 000	3, 000	. 01B, 0. 10Zr
V-19	Alumina	5	0	-----	C in charge	3, 000	3, 000	. 01B, 0. 10Zr
V-20	Magnesia	1	0	-----	C in charge	3, 000	3, 000	----------
[b] V-21	Magnesia	2	0	-----	C in charge	3, 000	3, 000	----------
V-24	Alumina	6	0	-----	C in charge	3, 000	3, 000	. 0025B

[a] Cast in tapered mold (other heats cast in straight mold).
[b] Melt-down time, 2 hr (other heats, 1 hr).

TABLE II

CRUCIBLE MATERIALS

Material	Brand name	Supplier	Chemical composition, weight percent								
			Al_2O_3	ZrO_2	MgO	SiO_2	CaO	Fe_2O_3	TiO_2	B_2O_3	Alkalies
Alumina	Taycor	The Charles Taylor's Sons Co.	87. 6	----	0. 04	11. 4	0. 03	0. 21	0. 07	Not detected	0. 41
Zirconia	Stabilized zirconia	Titanium Alloy Mfg. Div., National Lead Co.	. 02	93. 8	. 05	. 5	4. 9	. 02	. 63	Not detected	<. 01
Magnesia	Magnorite	Norton Co	----	----	97. 0	1. 5 to 2. 0	1. 3 to 1. 5	0. 1 to 0. 2	----	0.1 to 0.2	----

TABLE III

RESULTS OF CHEMICAL ANALYSIS OF HEATS

[Balance is nickel]

Heat	Crucible	Elements present, weight percent															
		Cr	Co	Mo	Ti	Al	Si	Mn	C	S	P	Zr	B	Ca	Mg	Fe	Cu
V-1	Zirconia	21. 2	14. 9	4. 00	2. 82	3. 30	0. 12	0. 13	0. 05	----	0. 003	0. 09	-----	-----	<0. 01	<0. 20	<0. 10
V-2	Zirconia	21. 7	14. 6	4. 00	3. 17	3. 45	. 14	<. 10	. 04	----	. 004	. 08	-----	-----	<. 01	<. 20	<. 10
V-3	Zirconia	20. 7	14. 8	4. 00	3. 22	3. 35	. 11	. 16	. 06	----	. 005	. 04	0. 0004	-----	<. 01	<. 20	<. 10
V-4	Zirconia	18. 1	15. 2	4. 10	2. 98	3. 10	. 10	. 10	. 05	----	. 006	. 06	. 0005	-----	<. 01	<. 30	<. 10
V-5	Zirconia	18. 2	15. 1	4. 20	3. 18	3. 15	. 10	. 10	. 09	----	. 008	. 09	-----	-----	<. 01	<. 30	<. 10
V-6	Zirconia	18. 8	15. 1	4. 15	3. 14	3. 14	. 10	<. 10	. 08	0. 008	. 003	. 19	. 0004	-----	-----	<. 30	-----
V-7	Zirconia	19. 4	15. 0	4. 10	3. 30	3. 35	. 14	. 15	. 08	----	. 006	<. 03	-----	-----	-----	<. 30	-----
V-8	Zirconia	19. 2	14. 5	4. 20	2. 98	3. 00	. 22	. 15	. 20	-----	. 007	<. 03	-----	-----	<. 01	-----	<. 10
V-8	Zirconia	19. 8	14. 5	4. 10	2. 98	2. 85	. 23	. 13	. 19	----	. 004	<. 03	. 0004	-----	<. 01	-----	<. 10
V-10	Zirconia	19. 8	15. 2	4. 10	3. 05	3. 15	. 12	. 10	. 13	----	. 005	. 06	-----	-----	<. 01	<. 30	<. 10
V-11	Magnesia	20. 0	16. 2	4. 20	3. 25	3. 58	. 18	. 10	. 05	----	. 004	<. 01	. 0017	-----	<. 01	<. 30	<. 10
V-12	Magnesia	20. 9	14. 8	4. 20	3. 15	3. 25	. 20	<. 10	. 10	----	. 004	<. 01	. 0089	-----	<. 01	<. 30	<. 10
V-13	Alumina	20. 4	14. 8	4. 20	3. 25	3. 37	. 25	. 12	. 05	----	. 007	<. 01	. 0003	<0. 01	<. 001	<. 01	<. 01
V-14	Zirconia	20. 8	14. 8	4. 20	3. 20	3. 30	. 19	. 11	. 09	----	. 007	. 01	. 0088	-----	<. 01	<. 30	<. 10
V-15	Alumina	19. 7	15. 0	3. 90	3. 08	3. 35	. 17	. 13	. 08	. 007	. 006	<. 01	. 0002	-----	<. 01	<. 30	<. 10
V-16	Alumina	20. 0	16. 0	3. 90	3. 12	3. 39	. 17	. 10	. 06	----	. 006	. 13	. 0009	-----	<. 01	<. 30	<. 10
V-17	Alumina	19. 4	16. 5	3. 75	3. 02	3. 26	. 16	. 12	. 07	----	. 008	<. 01	. 0074	-----	<. 01	<. 30	<. 10
V-18	Alumina	19. 8	15. 7	3. 70	3. 10	3. 26	. 12	. 13	. 07	----	. 006	. 09	. 0069	-----	<. 01	<. 30	<. 10
V-19	Alumina	20. 8	16. 0	3. 90	3. 17	3. 38	. 13	. 12	. 08	----	. 006	. 04	. 0090	-----	<. 01	<. 30	<. 10
V-20	Magnesia	----	----	----	----	----	---	----	. 12	----	. 007	----	. 0010	<. 01	<. 001	<. 01	<. 01
V-21	Magnesia	----	----	----	----	----	---	----	. 15	----	. 007	----	. 0004	<. 01	<. 001	<. 01	<. 01
V-24	Alumina	19. 8	15. 9	4. 05	2. 92	3. 06	. 16	<. 10	. 13	----	----	<. 01	. 0012	<. 10	<. 01	<. 30	-----

TABLE IV

STRESS RUPTURE DATA AT 1,600° F AND 25,000 PSI

[As-rolled bar stock was heat-treated 2 hours at 2,150° F and air-cooled unless otherwise noted; specimens were preheated 4 hours at test temperature before loading]

Heat	Crucible material	Rupture time, hr	Elongation, percent	Reduction of area, percent	Compositional variable, percent			
					C	Zr	B	Ti+Al
V–1	Zirconia	[a]82.3	------	5	0.05	0.09	------	6.12
		96.6	5	6				
V–2	Zirconia	117.7	8	3	.04	.08	------	6.62
		143.5	5	6				
V–3	Zirconia	90.7	4	4	.06	.04	0.0004	6.57
		126.0	5	4				
V–4	Zirconia	[a]99.5	6	4	.05	.06	.0005	6.08
		106.3	4	5				
V–5	Zirconia	[a]87.1	6	6	.09	.09	------	6.33
		91.2	5	6				
V–6	Zirconia	147.4	5	5	.08	.19	.0004	6.28
		133.7	6	8				
V–7	Zirconia	75.5	4	3	.08	<.03	------	6.65
		103.1	5	5				
V–8	Zirconia	81.2	8	12	.20	<.03	------	5.98
		66.3	11	9				
V–9	Zirconia	50.8	8	12	.19	<.03	.0004	5.78
		54.6	6	8				
V–10	Zirconia	85.5	9	9	.13	.06	------	6.20
		86.5	8	10				
		79.9	6	6				
		102.8	8	9				
V–11	Magnesia	185.2	3	2	.05	<.01	.0017	6.83
		229.9	5	5				
V–12	Magnesia	428.8	10	11	.10	<.01	.0089	6.40
		393.5	7	8				
V–13	Alumina	56.9	2	2	.05	<.01	.0003	6.62
		47.5	1	1				
V–14	Zirconia	666.3	17	16	.09	.01	.0088	6.50
		626.8	12	13				
V–15	Alumina	44.6	2	1	.08	<.01	.0002	6.43
		52.0	2	1				
V–16	Alumina	144.0	4	4	.06	.13	.0009	6.51
		118.9	4	4				
V–17	Alumina	400.4	7	6	.07	<.01	.0074	6.28
		346.0	7	5				
V–18	Alumina	243.8	7	6	.07	.09	.0069	6.36
		304.5	10	10				
V–19	Alumina	546.6	11	12	.08	.04	.0090	6.55
V–20	Magnesia, first heat	225.2	5	4	.12	<.01	.0010	------
		206.9	4	3				
V–21	Magnesia, second heat	103.4	4	2	.15	<.01	.0004	------
		106.0	3	2				
V–24	Alumina	170.0	5	3	------	<.01	.0012	5.98

[a] Heat-treated 1 hr at 2,150° F, air-cooled.

TABLE V

CREEP-RUPTURE DATA AT 1,600° F

[Initial condition: 2 hr at 2,150° F, air-cooled, plus 4-hr preheat at 1,600° F before loading]

Heat	Stress, psi	Minimum second-stage creep rate, percent/hr	Rupture			Interruption	
			Time, hr	Elongation, percent	Reduction of area, percent	Time, hr	Total deformation, percent
V-15	25,000	0.0160	45	2	1	----------	----------
		.0060	52	2	1	----------	----------
	20,000	0.0070	158	3	2	----------	----------
		.0040	--------	--------	--------	165	1.23
		.0058	--------	--------	--------	117	1.00
		.0046	--------	--------	--------	85	.76
		.0052	--------	--------	--------	85	.76
		.0084	--------	--------	--------	47	.55
		.0058	--------	--------	--------	23	.29
V-6	25,000	0.0036	147	5	5	--------	--------
		.0095	134	6	8	--------	--------
	22,500	0.0032	208	5	4	--------	--------
		.0036	--------	--------	--------	172	1.25
	20,000	0.0027	--------	--------	--------	165	0.63
V-12	28,000	0.0025	296	10	14	--------	--------
		.0040	--------	--------	--------	214	3.45
		----------	--------	--------	--------	188	1.21
		.0046	--------	--------	--------	68	.56
	25,000	0.0018	429	10	11	--------	--------
		----------	394	7	8	--------	--------
	20,000	Negative	--------	--------	--------	165	0.15
V-14	30,000	0.0021	266	8	9	--------	--------
		----------	--------	--------	--------	214	1.18
	25,000	0.0004	666	17	16	--------	--------
		.0003	627	12	13	--------	--------
	20,000	Negative	--------	--------	--------	165	0.04

TABLE VI

MICROSTRUCTURAL FEATURES OF SPECIMENS AFTER AGING UNDER STRESS AT 1,600° F

Condition	Heat V–15				Heat V–6				Heat V–12				Heat V–14			
	Nodules (a)	γ' density (b)	Depleted grain boundaries (c)	Microcracks (d)	Nodules (a)	γ' density (b)	Depleted grain boundaries (c)	Microcracks (d)	Nodules (a)	γ' density (b)	Depleted grain boundaries (c)	Microcracks (d)	Nodules (a)	γ' density (b)	Depleted grain boundaries (c)	Microcracks (d)
Approximately equal-strain-rate study																
0.3 percent creep deformation	239	---	49	5	---	---	---	---	---	---	---	----	---	---	----	----
0.6 percent creep deformation	301	---	76	17	---	---	---	---	5	---	2	2	---	---	----	----
0.8 percent creep deformation	332	---	184	34	---	---	---	---	---	---	---	----	---	---	----	----
1.0 percent creep deformation	288	---	173	31	---	---	---	---	---	---	---	----	---	---	----	----
1.2 percent creep deformation	334	---	151	118	---	---	---	---	---	---	---	----	---	---	----	----
3.5 percent creep deformation	418	134	264	314	175	137	127	78	63	157	60	30	20	117	23	2
Ruptured	---	---	---	---	---	---	---	---	79	---	165	77	---	---	----	----
	532	---	764	958	228	---	568	532	176	---	676	243	86	---	538	198
Equal-stress study																
165 hr at 20,000 psi	418	134	264	314	129	151	72	9	25	158	16	None detected	0	125	None detected	None detected
Ruptured at 25,000 psi	225	256	192	374	254	109	916	145	145	67	442	166	86	51	661	402
	218	---	211	378	---	---	---	---	---	---	---	----	90	---	530	330

[a] Mixed carbide and γ' nodule with greater than 5-micron diam., number in 0.008 sq in.
[b] Number of γ' particles per sq in. at 12,000 diam.
[c] Grain boundaries where depletion was detected at 1,000 diam., number in 0.008 sq in.
[d] Microcracks detected at 1,000 diam., number in 0.008 sq in.

TABLE VII

MICROSTRUCTURAL FEATURES OF SPECIMENS AGED WITHOUT STRESS AT 1,600° F

Aging time, hr	Heat V–15			Heat V–6			Heat V–12			Heat V–14		
	DPH	Nodules (a)	γ' density (b)	DPH	Nodules (a)	γ' density (b)	DPH	Nodules (a)	γ' density (b)	DPH	Nodules (a)	γ' density (b)
0.5	359	---	---	354	---	---	357	---	---	373	---	---
1	364	---	---	362	---	---	362	---	---	380	---	---
4	359	---	---	353	---	---	357	---	---	366	---	---
10	355	45	588	348	32	544	348	16	768	362	0	584
100	345	180	134	346	57	147	346	33	168	355	19	137
188	338	---	107	342	---	116	340	---	101	353	---	103
500	335	300	65	344	139	67	339	149	68	344	25	64

[a] Nodules with greater than 5-micron diam., number in 0.008 sq in.
[b] Number of γ' particles per sq in. at 12,000 diam.

U.S. GOVERNMENT PRINTING OFFICE: 1960